Part IV

WINDS AND DISK-CORONA OSCILLATIONS

Advective Flow Paradigm And Microquasar GRS1915+105

Sandip K. Chakrabarti
SNBNCBS, JD Block, Salt Lake, Calcutta 700098

Abstract. Advective accretion disks and winds are the most self-consistent solutions today. We describe this paradigm briefly and show how it attempts to explain some of the interesting observations of the galactic microquasar GRS1915+105.

Keywords: black hole physics, jet, accretion, GRS 1915+105

1. Introduction

The standard accretion disk model of Shakura and Sunyaev (1973) was modified immediately after it was proposed. The spectrum of black hole candidate Cyg X-1 showed (Sunyaev and Trümper, 1979) that apart from the modified cool black body spectrum, it also exhibits a power-law emission at much higher energies, indicating the presence of electrons much hotter than a standard disk. Subsequently, Sunyaev and Titarchuk (1980) showed that the power-law emission is the result of the Comptonization of soft photons from a standard disk by hot electrons whose source was thought to be *outside* the standard disk, be it in the form of floating 'Compton clouds' or 'magnetic corona'.

Meanwhile, transonic flow models were developed in the early eighties (Muchotrzeb and Paczyński, 1982, Matsumoto et al. 1984) to modify inner edge of the standard disk to ensure that it passes through a sonic point. These solutions ensure that the specific energy of the flow remains negative as in a Keplerian disk. However, there is another class of transonic disk solutions which are the generalizations of the classical Bondi (1952) solutions when angular momentum, viscosity, heating, cooling etc. were taken into account. These are known as advective flow solutions (Chakrabarti, 1990, 1996a, 1998ab, 2000a). Particularly interesting is that these solutions did away with the external Compton clouds as the inner sub-Keplerian region itself is found to behave like one for all practical purposes.

In this review, I briefly present these solutions for viscous and non-viscous flows. The solutions can be suitably combined to obtain a paradigm of the black hole astrophysics. Truly speaking, a cool, Keplerian disk with a negative energy cannot smoothly join to most of these *steady* solutions which require positive energy (at least in quasi-adiabatic flows). For time-dependent flows such restrictions do not apply. In fact, steady transition from a Keplerian disk to an advective disk may require systematic heating of a Keplerian disk or the assumption that all disks are fundamentally non-steady, only the time scale varies. We also try to explain some of the observed features of the galactic micro-quasar GRS1915+105. We find that it always helps to keep a paradigm in the back of one's mind while attempting to explain any observations. Otherwise, each observational feature would demand a separate 'model' which may or may not fit with the global solutions of accretion and winds.

2. Advective Flow Paradigm

2.0. Hydrodynamic and magnetohydrodynamic flows

Though most of the literature concentrates on disks and jets separately, it is advisable (and *economical*) to study them simultaneously. This is because in global studies, always both types of solutions appear together. Examples are Bondi (1952) and generalized Bondi solutions (Chakrabarti, 1990; 1996bc). Numerical simulations have also shown outflows in much of the region of the parameter space (Molteni, Lanzafame & Chakrabarti, 1994 [MLC94]; Molteni, Ryu & Chakrabarti, 1996 [MRC96]; Ryu, Chakrabarti & Molteni, 1997 [RCM97]). Figure 1 shows the broad classification of all possible steady, inviscid solutions of advective disks (adapted from Chakrabarti, 2000a). Solutions shown are obtained for inviscid adiabatic flows (Chakrabarti 1989, 1996b) but they remain valid close to the black hole even when these conditions are relaxed. One important aspect which requires emphasizing is the presence of a centrifugal pressure supported boundary layer (CENBOL) in some of these steady solutions and in most of the non-steady solutions! Rapid inflow keeps the angular momentum to an almost constant value. Thus, centrifugal force becomes a dominant force. It slows downs matter in this barrier, heats them up so that hard X-rays could come out and finally drives hot matter perpendicular to the disk to form outflows. The barrier even oscillates with a large amplitude if conditions are right (Molteni, Sponholz & Chakrabarti, 1996; RCM97) thereby giving rise to quasi-periodic oscillations of X-rays. Beside each solution in Fig. 1 schematic picture is given of accretion and outflows. Inward and outward pointing arrows indicate accretion wind solutions respectively. In (A) and (a), low energy and low angular momentum flow behaves like a conical Bondi inflow and Parker type winds well known in solar physics. In (B) and (b), a steady shock does not form, the inflow becomes hotter due to slowing down at the centrifugal barrier. Numerical simulation shows that an oscillating shock forms (RCM97) which is accompanied by a non-steady outflow. In (C) and (c), the steady inflow solution has a standing shock. This has been tested by numerical simulations (Chakrabarti & Molteni, 1993 [CM93]; MLC94; MRC96). Positive energy outflow is also found to be steady. In (D) and (d), the inflow passes through an inner sonic point, but the outflow forms a steady shock (CM93). In (E) and (e), no shock is possible in the steady solution though there are three sonic points and we feel that *non-steady* shocks would form. In (F) and (f), both the inflow and the outflow have no shocks, and energetic steady solutions are present as both pass through the inner sonic point. In (G) and (H), solutions are incomplete since they are not from infinity to the horizon. Thus, no steady solution is possible. Simulations (Ryu and Chakrabarti, 1996) indicated that flow is highly unsteady in these cases which are schematically shown in panels (g) and (h) respectively. Especially interesting is the solution of O$*$, where disks could be 'thick' not because of gas or radiation pressure, but because of turbulent pressure. Solutions from (g) are with negative energy.

When viscosity is present, closed topologies open up to join with Keplerian disks and when heating (such as magnetic, viscous) flow from a Keplerian disk can pass through shocks and sonic points (Chakrabarti 1990, 1996, 2000a). For instance, solutions in (C) become similar to those of (I) and (i) while those in I* become similar to those of (J) and (j). These solutions are the backbones of the advective disk paradigm and are useful in obtaining complete solutions of the disk/jet systems. When magnetic field is added, the flow passes through the fast and the slow magnetosonic point and the Alfv́en point. Possible outflowing solutions with or without shocks have been presented in Chakrabarti (1990). It is likely that in some regions of the parameter space, these magnetohydrodynamic shocks should also show oscillations.

2.0. Effects of Radiative Transfer

Fully self-consistent two temperature flow in the advective disks was studied very recently. Chakrabarti & Titarchuk (1995) computed temperatures of electrons and ions for various accretion rate parameters in the CENBOL region and found that for high Keplerian rate CENBOL cools down completely and shock disappears. Soft photons intercepted by CENBOL are reprocessed by hot electrons to produce hard X-rays which are observed as a power-law tail in the hard states. In soft states, the hard tail is formed due to bulk motion Comptonization.

Hot CENBOL drives outflows from the disk along the vertical axis. When the outflow rate is very high, the sonic sphere (i.e., region of the wind till its first sonic surface) becomes dense enough to cool down due

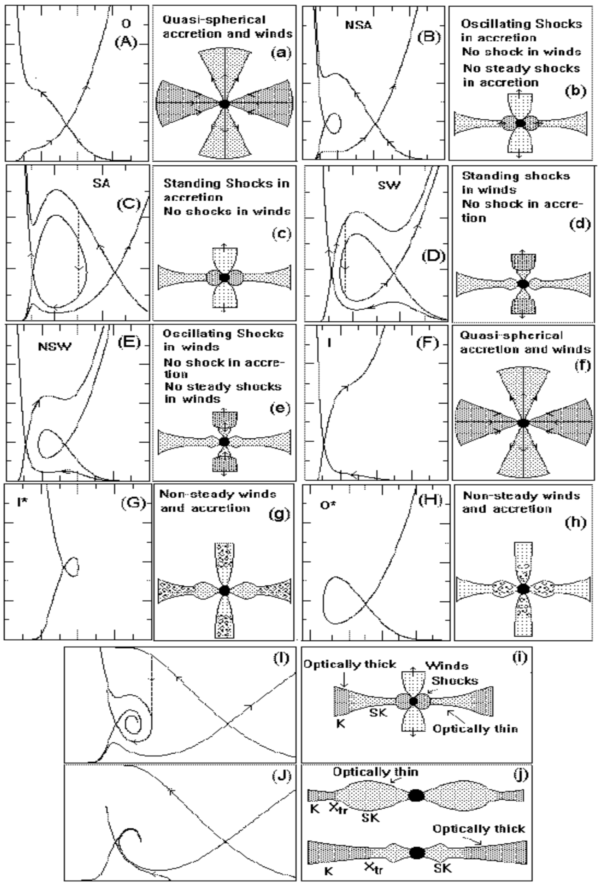

Figure 1. Nature of the solutions (Mach number along Y-direction and logarithmic radial distance along X-direction) of inviscid (A-H) and viscous (I-J) advective disks. Schematic flow behaviour of these solutions in meridional plane are shown in (a-j). Shock locations (C, D) and incomplete solutions (G, H) are indicated by puffed up (c, d) and turbulent regions (g, h) respectively. Solutions with three sonic points having no steady shock are shown oscillating with arrows at both ends (b, e).

to Comptonization by the soft photons from the Keplerian disk. Estimation of the rate of wind generation (Chakrabarti 1998ab, Chakrabarti 1999a) shows that in purely soft states no outflow is possible and in purely hard states, outflow is very small. Thus above mentioned cooling of the sonic sphere is not possible. When compression ratio of the shock is intermediate, outflow rate is significant.

After the sonic sphere is cooled sonic surface comes closer to the black hole and matter below it returns back to the disk, while matter

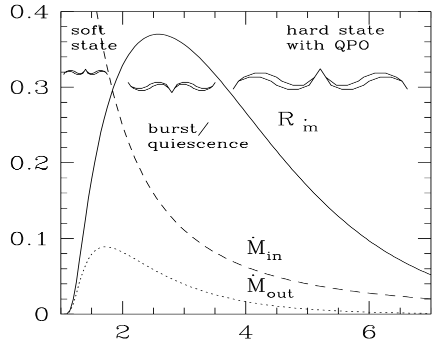

Figure 2. Variation of ratio of outflow and inflow rates as a function of the compression ratio at the accretion shock. Also shown are expected outflow rate (short-dashed curve) for a given inflow rate (long-dashed curve).

above it separates as blobs. Thus blobby jets are expected in this intermediate states (this may also be called flare/quiescence or On/Off transition states). The return flow acts as a feedback on the already accreting flow and the count rate undergoes very interesting behaviour. Fig. 2 (Chakrabarti, 2000b) shows how the ratio ($R_{\dot m}$) of the outflow rate $\dot M_{out}$ and the inflow rate ($\dot M_{in}$ assumed to be proportional to $1/R^2$; $R \rightarrow 1 \rightarrow$ soft state; $R \rightarrow 7 \rightarrow$ hard state) depend on the compression ratio R of the gas at the shock. This clearly shows that there is a distinct relation between the spectral states and the outflow rate.

An important characteristics the spectrum should show is that spectral slops of the power-law component should be harder in soft states and softer in the hard states. This is because, in the hard states, outflows from CENBOL reduced electron density but the soft-photon intensity from the pre-CENBOL flow remains the same. This softens the spectra in hard states (Chakrabarti, 1998c). Similarly return flow hardens the spectrum. A corollary of these effects is that the pivotal point of the power-law tail shifts to a larger energy in presence of winds/return flows.

3. Explanations of Observational Aspects of GRS1915+105

GRS1915+105 exhibits very intriguing light curves. Belloni et al. (2000, hereafter B00) divided them into twelve types. They draw HR1 vs HR2 diagrams where HR1=B/A and HR2=C/A (A:2-5keV, B:5-13keV, C:13-60keV). Color-Color diagrams showed very intricate structures (shapes of atoll, banana, etc.). If the pre-shock flow is indeed the source of the soft photons, photons originating in (0-3) keV range should be roughly proportional to the Keplerian accretion rate. Thus, photon number may show time variation (due to periodic changes in the 'accretion rate' due to return flow mentioned above). However, no QPO should be seen from these photons. Chakrabarti & Manickam (2000, hereafter CM00) demonstrated this (see also, Rao et al. 2000). The harder photons ($E > 3$ keV) would usually come from the post-shock flow. Since the spectra intersect at around 17keV, and for $E > 17$keV, photon number is not large, we make our choice of A, B and C to be in ranges of $(0-3)$ keV, $(3-17)$ keV and $(17-60)$ keV respectively (B and C would be related to sub-Keplerian rate). According to our paradigm, roughly speaking, A, B and C should be proportional to each other (since B and C are produced by interception of soft photons measuring A. Of course, soft X-ray absorption makes matter more complex.) and whenever hardness or softness ratios are plotted basically straight lines are expected, instead of Atoll, Banana and Z shapes. The results are presented in Nandi et al. (2000a) and the details of the physical interpretations are presented in Manickam et al. (2000).

One important conclusion of Belloni et al. (2000) was that the disk apparently has three states: A (low rate and low HR1, HR2), B (high rate, high HR1) and C (low rate, low HR1, variable HR2 depending on length of the event). It seems that the State C exhibits QPO. State A and state B do not exhibit QPO. More interestingly, except for $C \rightarrow B$ transition, all other transitions of states are allowed. Nandi et al (2000b) found evidence of QPO in some of the State A light curve.

As discussed in Chakrabarti (2000ab) there are practically four distinct ways that the solutions in Fig. 1 could be combined for a realistic accretion-wind system. If the accretion rate is very low and shock does not develop, QPO may not be seen. In GRS 1915+105 we need not be concerned with this type of flow. The remaining three are shown in Fig. 3 (Chakrabarti et al. 2000a). If the shock develops, QPO would be seen but wind may be negligible or absent depending on the compression ratio of the shock. The object would be in State C of B00 or hard class of Nandi et al. (2000). If the accretion rate is generally increased, shock is weakened (compression ratio goes down), and in the intermediate state, burst/quiescence or On/Off may be seen. There could be two types of 'On' states (State A and State B of B00). After the winds of State C fills in the sonic sphere and cools it down by Comptonization, CENBOL and the region till the sonic sphere collapse. This is the State A of B00. Now there are two possibilities (Chakrabarti, 1999b) either the flow separates completely as a blob and returns to State C or the flow mostly return back to the accretion disk and enhances the

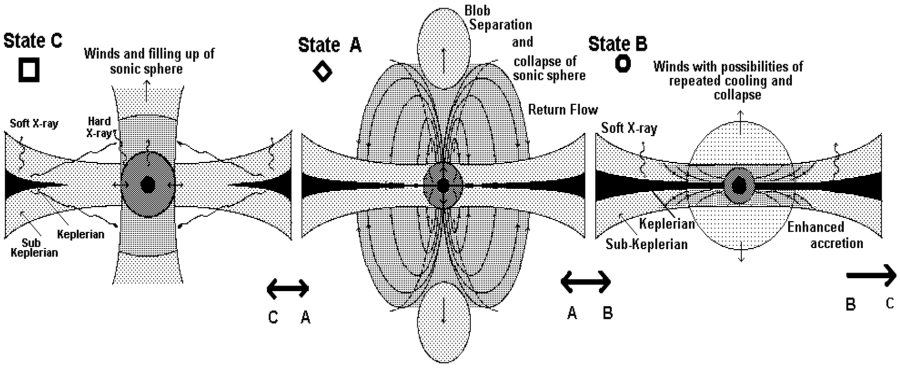

Figure 3. Suggested accretion/wind configurations in States A, B and C of B00.

accretion. This would be the State B of B00. This may in turn increases the outflow (see, Fig. 2). But shock itself is getting weakened because of post-shock cooling, hence the outflow is very mild, but may be in a threshold so that a bit more outflow can cause the sonic sphere to collapse again. Thus, occasional trips to State A from State B is possible. Once enhanced matter is drained out and the shock bounces back to roughly the original location (compatible with its specific energy and angular momentum) State C forms again. Since State C produce fewer soft photons, State B is not directly possible from State C without first producing return flow and enhanced accretion. This may explain why a transition from C to B is difficult.

Among other confirmations of our paradigm, we note that Nandi et al. (2000b) demonstrated that the spectral slopes of GRS 1915+105 are hardened by enhanced accretion and softened by return flows. CM00 found that the duration of the Off states strongly depend on QPO frequency. Dhawan et al (2000) observationally demonstrates that jets originate from what we term CENBOL region.

4. Concluding remarks

Advective disk paradigm being made up of the most complete accretion disk/wind solutions, it is not surprising that most of the observations could be explained by this paradigm. However, our explanations of the light curves of GRS 1915+105 have been over simplified since we ignored the effects of magnetic fields altogether. Apart from a new spectral component due to synchrotron radiation and perhaps increasing the outflow velocity to a much larger value, no other effect is expected as far as our State description is concerned.

This work is partly supported by a grant from ISRO for the project 'Quasi-Periodic Oscillations of Black Holes'.

References

Belloni, T., Wolt, M-K, Méndez, M., van Der Klis M. and van Paradijs J., 2000, *Astron. Astrophys.* 355 271

Bondi, H. 1952, *Mon. Not. R. Astron. Soc.*, 112, 195

Chakrabarti, S.K., 1989, *Astrophys. J.*, 347, 365

Chakrabarti, S.K., 1990, *Theory of Transonic Astrophysical Flows*, World Scientific (Singapore)

Chakrabarti, S.K., 1996a *Phys. Rep.*, 266, 229

Chakrabarti, S.K., 1996b, *Mon. Not. R. Astron. Soc.*, 283, 325

Chakrabarti, S.K., 1996c, *Astrophys. J.*, 464, 664

Chakrabarti, S.K., 1998a, *Ind. J. Phys. (Reviews)*, 72B, 565

Chakrabarti, S.K., 1998b, *Observational Evidence for Black Holes in the Universe*, 19, Kluwer Academic Publishers (Holland).

Chakrabarti, S.K., 1998c, *Ind. J. Phys.*, 72B, 565

Chakrabarti, S.K., 1999a, *Astron. Astrophys.*, 351, 185

Chakrabarti, S.K. 1999b, *Ind. J. Phys.*, 73B, 931

Chakrabarti, S.K. 2000a, *Nuovo Cimento* (in press).

Chakrabarti, S.K. 2000b, *Proceedings of the Heidelberg Workshop on High Energy Gamma-Ray Astronomy*, eds. F.A. Aharonian and H. Völk.

Chakrabarti, S.K. and Molteni, D. 1993, *Astrophys. J.*, 417, 671 [CM93]

Chakrabarti, S.K. and Manickam S.G., 2000, *Astrophys. J. Lett.*, 531, L41 [CM00]

Chakrabarti, S.K. and Nandi, A. 2000a, *Ind. J. Phys.* (submitted).

Chakrabarti, S.K. and Titarchuk, L.G., 1985, *Astrophys. J.*, 455, 623

Dhawan V., Mirabel I.F. and Rodríguez L.F., 2000, *Astrophys. J.*, *submitted.*

Manickam, S.G., Nandi, A. and Chakrabarti, S.K., 2000, *Astron. Astrophys.* (in preparation)

Matsumoto, R., Kato, S., Fukue, J. and Okazaki, A.T. 1984, *Publ. Astron. Soc. Japan*, 36, 71

Molteni, D., Lanzafame, G. and Chakrabarti, S.K., 1994, *Astrophys. J.* 425, 161 [MLC94]

Molteni, D., Ryu D. and Chakrabarti, S.K., 1996, *Astrophys. J.* 470, 460 [MRC96]

Molteni, D., Sponholz, H. and Chakrabarti, S.K., 1996, *Astrophys. J.*, 457, 805

Muchotrzeb, B. and Paczyński, B. 1982, *Acta Astron.*, 32, 1

Nandi, A., Manickam, L.G. and Chakrabarti, S.K., 2000a, *Ind. J. Phys.* (in press)

Nandi, A., Manickam, L.G. and Chakrabarti, S.K., 2000b, *Mon. Not. R. Astron. Soc.* (submitted)

Rao, A.R., Naik, S., S.V. Vadawale and S.K. Chakrabarti, 2000, *Astron. Astrophys.* 360, L25

Ryu, D., Chakrabarti, S.K. and Molteni, D., 1997, *Astrophys. J.*, 474, 378 [RCM97]

Ryu, D. and Chakrabarti, S.K. 1996 (unpublished)

Shakura, N.I. and Sunyaev, R.A. 1973 *Astron. Astrophys.* 24, 337

Sunyaev, R.A., and Trümper, J. 1979, Nature, 279, 506

Sunyaev, R.A. and Titarchuk, L.G., 1980, *Astron. Astrophys.* 86, 121

A Review of Disk-Corona Oscillations

Jean Swank
NASA/Goddard Space Flight Center

Abstract. Low frequency ($\approx 0.1 - 35$ Hz) quasi-periodic oscillations of the X-ray flux characterize many of the black hole candidates, in particular those which have radio evidence for jets. These QPO have amplitudes of up to 20 % in the states of black hole novae which are called very high and intermediate and are correlated with the break frequency of the band-limited low frequency white noise. With transition to the state called the soft high state, both the QPO and the noise disappear. While the noise is strong in the low hard states like that of Cyg X-1, the QPO, when present, are weak and broad. In their strong manifestations, these QPO have the curious property of appearing to have the spectrum of the power-law component which dominates in the low state, while correlations between their frequency and the disk component in the spectrum imply control by the disk. The correlations, the harmonic structure of the QPO, and the phase lags have complex behavior in the same source (GRS 1915+105, XTE J1550-564). The phenomena point to interaction between the disk and the corona, for which there are several interesting ideas.

Keywords: quasi-periodic oscillations, microquasar, black hole candidates

1. Introduction

Disk-corona oscillations, as discussed in this paper, refer to the oscillations in X-ray flux, appearing as quasi-periodic oscillations (QPO) in the power density spectra, which are in the non-thermal spectra possibly originating in a corona, but which appear to be related to optically-thick emission associated with the accretion disk. The QPO can have an amplitude of 10–20 %. In the power density spectra of black hole candidates (BHCs), a subset of which are known to be microquasars, several low frequency features have appeared. For a given source several QPOs can appear simultaneously, in which case it is clear that there are more than one phenomenon manifested. The characteristics of the features seen in the range 1–15 Hz are best known, but they have been seen below 1 Hz and above 15 Hz.

These oscillations were seen with *Ginga* in GX 339–4 (Miyamoto et al. 1991) and Nova Muscae (Takizawa et al. 1997). The frequencies increased with the source intensity, not always in the same way. When *RXTE* discovered GRS 1915+105 to be active in 1996, the oscillations were soon found to be prominent during long episodes of hard flux and relative quiescence, and the oscillation frequencies were found to be strongly correlated with the source intensity (Chen et al. 1997).

GRO J1655–40 became active and showed the same kind of features (Remillard et al. 1999). By the end of 1999, *RXTE* had observed recurrences of the black hole candidate transient 4U 1630–47, and 4 new transients, all of which exhibited at some stages very high amplitude low frequency QPOs: GRS 1739–278, XTE J1748–288, XTE J1550–564, and XTE J1859+226.

Cyg X–1, 1E 1740.7–2942, GRS 1758–258, and several transient sources which did not get very bright, have been known for band limited white noise. Sometimes there have been peaks and even a harmonic in the frequency range where the spectra roll over (Cui et al. 1997; Smith et al. 1997). These have lower amplitudes, 5 %, and sometimes are hard to distinguish from a sharp transition in the power density spectrum. In Cyg X–1 the amplitude was highest during the transitions between low and high states, appropriately called the "intermediate state".

2. Characteristics of the QPO

Usually the QPO feature has at least one harmonic. Sometimes a peak at what would be the subharmonic is present. For simplicity we refer to the dominant peak as representing the phenomenon, whatever may be the real fundamental of the oscillation.

Almost always it is present over a range of luminosities and the frequency varies with luminosity. In most cases the frequency has increased with count rate and indeed with luminosity, when the spectrum has been taken into account. GRO J1655–40 was a notable exception, with the frequency generally decreasing with the total luminosity. However, Sobczak et al. (2000) found that frequency was positively correlated with the flux of the soft spectral component. There may be some counter-examples. In 4U 1630–47, a square wave oscillation of flux at a lower frequency was observed (Dieters et al. 2000) and two low frequency QPOs were observed in the 1-10 Hz range, one moving with the flux, the other stationary. These frequencies are at least a factor of 10 too low to be related to the inner most stable orbit of the accretion disk, for which the Kepler frequency would be 2200 Hz $(M/M_{\odot})^{-1}$.

The energy spectra of the sources can usually be well or almost described by an optically thick component and a non-thermal component. A physical model would be a disk spectrum Comptonized in a hot corona, but it can be approximated by the a multicolored disk and a power-law. The QPO usually appears when the flux is dominated by a relatively hard power-law-like component.

The energy spectrum of the QPO fundamental is that of the power-law component. Cui et al. (1999) plot (for XTE J1550–564) the root mean square (rms) amplitude of the QPO fundamental and harmonic with energy. The fundamental tracks the energy spectrum. Curiously the harmonic reverses and declines with energy, in comparison.

It was shown (Wijnands & van der Klis 1999b) that for a number of observations of BHCs, the break frequency of the band limited white noise component was about a fifth of the QPO frequency. However Morgan et al. (1997) exhibit power density spectra with the QPO frequency clearly corresponding to the break frequency. The exact connection between the two requires further study.

For GRS 1915+105 there is a great deal of data from different states and correlations between characteristics have been studied with several approaches. Markwardt et al. (1999) looked at many observations in which on time scales of minutes, the flux varied strongly (factors of 2-10). They averaged power spectra for given flux levels and found that the average exhibited a strong correlation of frequency of the QPO with the bolometric flux of the disk component in a spectral fit (4 s spectra), above the frequency of about 4 Hz. Muno et al. (1999) computed spectral parameters and power spectra for 16 s intervals of a larger set of observations, including those in which variations were slow. Frequency appears correlated with disk inner temperature for many of these. Plots with respect to disk black body flux, temperature, and inner radius all show runs of correlated data points, but also subsets clearly violating the correlation or having a very different correlation, indicating the behavior is not unique.

It is tempting to think of the frequency as related to the Kepler frequency at some radius, although the factor and physical origin of the relation may not be clear. Trudolyubov et al. (2000) leapfrog from the dependences of f_K and the viscous time scale at the radius to the relation between the duration of the hard state and the minimum frequency observed. The duration and frequency are easy to measure. The inner radius of the disk is difficult to measure, especially when the disk inner temperature appears to be low and the radius large, so that the *RXTE* PCA can only "see" the Wien tail of the energy spectrum. This gives $t \propto f_K^{-7/3}$ with a proportionality depending on the rate of mass flow through the shell. For the sets of observations with hard dips, this correlation appears to be a good fit. For the observations with soft dips, the dependence is significantly steeper.

For a given mass accretion rate in the disk, the temperature has a constrained relation to the radius, of course. Belloni et al. (2000) examined whether this relation holds and allows identification of the mass flow in the disk. Their aim was to compare to the mass loss rate in the radio emitting plasma that is ejected. These questions are just the sort that can give physical insight into the correct description of the disk accretion and the generation of winds and jets, but the X-ray calibration to date limits the conclusions.

The confusion of opposite dependence between frequency and total count rate in GRO J1655–40 and GRS 1915+105 appeared clarified by their having similar correlation with the disk flux alone. Furthermore, Sobczak et al. (2000) found that for XTE J1550–564, while the dependence of the QPO frequency with either temperature or radius was complex, the frequency did increase with disk flux. But from the point of view of the Accretion Ejection Instability (Tagger & Pellat 1999; Rodriguez et al. 2000) the complex dependence of the QPO frequency on radius is just what would be expected if the inner disk of GRO J1655–40 is nearer to the black hole, where relativistic effects can cause a turnover of the curve.

To interpret these correlations, physical models are needed for which the data can determine the parameters reliably. In deducing radii of the disk, even with the caveat that it is the optically thick disk, we are using zero-order approximations, when we know that we should consider the scattering atmosphere of the disk together with advective and wind flows (Merloni et al. 2000). However, although the meaning of the slopes may need modification, the fits to the data show that correlated changes occur, with values of the parameters often in realistic ranges.

3. Relation of Disk-Corona Oscillations to other QPO

Although much of the discussion has been in terms of the inner radius of an optically thick accretion disk that is being seen in the X-ray spectrum, it should be remembered that the QPO has appeared to occur simultaneously with the QPO that appears at much higher frequencies. It has seemed reasonable that the latter could reflect either the Kepler orbital frequency near the Innermost Stable Circular Orbit about black holes or the eigenfrequency of the fundamental modes of oscillation of the inner disk. High frequencies have been reported for 5 BHCs. For GRO J1655–40, XTE J1550–564, and XTE J1859+226, they have occurred together. Obviously if the higher frequency reflects emission from near the inner edge of the disk, the lower frequency cannot be the same thing, although it could be a different time scale at the same place. Alternatively, the inner disk may not be otherwise seen directly, while the lower frequency could reflect a transition region in the disk rather than the inner radius.

For GX 339–4 and GRS 1739–278 the low frequencies were only seen around 6 Hz and 5 Hz respectively. For Nova Muscae, GRS 1915+105, XTE J1550–564, 4U 1630–47, XTE J1859+226, values sampled include similar ranges within 0.08-18 Hz, while the high frequencies of the last 4 of these were 67 Hz, 161-237 Hz, 185 Hz, and 150-200 Hz. For two of the sources, GRO J1655–40 and XTE J1748–288, the low frequencies were higher, 14-35 Hz. GRO J1655–40's high frequency was also higher, 300-400 Hz. Dynamical masses are so far known only for GRO J1655–40 and Nova Muscae. How the frequencies scale with black hole mass is not yet clear.

QPOs at frequencies an order of magnitude below these disk-corona oscillations also occur. One type of variation which generates very low frequency oscillations in the power spectra are square-wave modulations of the flux originally called "flip-flops" by Miyamoto et al. (1991), and also dips. GRS 1915+105 has a 15 mHz feature whose folded light curve looks almost like an occultation (Morgan et al. 1997).

The disk-corona oscillation is in a frequency range just below the Horizontal Branch Oscillations (HBO) of Low Mass Binary Neutron Stars and they can look similar in harmonic structure. Usually the amplitude is lower. The HBO and Normal Branch frequencies of the Atoll and Z sources have been found to be correlated to the lower of two kilohertz frequencies. For the BHCs, Psaltis et al. (1999) see features, sometimes very broad, that they consider to be counterparts of the neutron star lower kilohertz frequency. They find the disk-corona oscillation and this oscillation to be related in the same way as are the HBO and the lower kilohertz oscillation. The ratio of the average lower frequency in the BHCs and of the HBO in the neutron star sources could be consistent with being inversely proportional to the mass of the compact object (Chen et al. 1997).

4. Relation to Black Hole Accretion States

Most black hole candidate transients have outbursts which last several months, but not as long as has GRS 1915+105. They usually have a well defined onset, rise, peak, and decay, although there are rather frequently one or more brightenings during the decay. GRS 1915+105 has for several years now evolved from one recurrence to another. GRO J1655–40 and XTE J1550–560 recurred after a year, but they had clearly gone into quiescence first. In a typical case there is a rising phase, frequently a very high state (VHS), a high soft state (HS) and decay through an intermediate state (IS) to a low hard state (LS) and finally a quiescent state.

RXTE has had a number of successful observations of rising phases (XTE J1550–564, Cui et al. 1999; 4U 1630–47, Dieters et al. 2000; XTE J1859+226, Markwardt et al. 1999) In these cases the spectra started out harder than achieved subsequently in the outburst. The spectrum softens as the flux rises. The disk-corona oscillation starts below 1 Hz with high amplitude and rises in frequency, increasing in width and decreasing in amplitude somewhat. But the time scale for these changes is days rather than the minutes required for the GRS 1915+105 hard dip recoveries.

At the end of the rising phase, the transient may be in the VHS with a strong power law and a strong disk flux. In both the VHS and IS the QPO is present. In the HS the soft component is very bright (several tenths of the Eddington limit). A relatively steep power-law component extending to high energy may be of a completely different origin than the Compton up scattering in a hot corona that is favored for explaining the VHS. There are NO QPOs in the HS.

In the case of GRS1915+105, we discuss a scenario of mass flow in the disk, removal of the disk into a corona and ejection into jets. Does this scenario apply to the transient outbursts? In the VHS there is outflow, because the radio emission often starts sometime during the rising phase. The mass accretion rate in the outer disk is large and the inner radius of the disk is large. As the mass flow rate subsides the disk collapses to be optically thick, or at least it is optically thick farther in toward the center. At a lower rate, there are also radio injections associated with the transitions to the HS and out of it to the IS (e.g. Hjellming et al. 2000) from comparison of the radio and X-ray transitions (for XTE J1748–288 and XTE J1859+226). This scenario would imply that spectral fits obtain larger inner radii for the disk in the VHS than in the HS, but only a factor of 2 seems to have been observed. Much needs to be done to understand the evolution.

5. Explanations for the Low Frequency QPO

The flux that is oscillating appears to be the hard power-law component of the spectrum, the candidate for indicating the presence of a hot corona. The thermal photons from the disk would be the dominant source of the seed photons to be up-scattered in the corona. Whether the corona is spherical and central or extended over the inner disk, or whether there is simultaneously spherical infall is not clear. Radio observations are indicating (See Fender, this volume) outflow and synchrotron radiation. A number of models have been suggested and would explain some of the observations. I only mention some of the ideas.

Disk-corona oscillations are probably not like the possible coronal radial infall oscillations suggested for the normal branch oscillations at about 6 Hz in the neutron star Z sources. Neither observations or simulations show the large amplitude and variability.

It has been suggested that the HBO in neutron stars are due to the Lense-Thirring frame dragging in the strong gravitational field close to rather heavy neutron stars (twice the nodal precession frquency of slightly tilted and elliptical orbits.) Systematic similarity of the neutron stars and BHCs has been claimed, as mentioned above. In some cases the approximately linear relation between two frequencies in the BHCs and the HBO and lower kilohertz frequencies for the neutron stars is impressive. Psaltis & Norman (2000) have made a case that the frequencies observed are the resonant frequencies in the disk, whatever the mechanism for modulating the X-ray flux.

One idea that appears to generate the right order of magnitude of frequencies and similar dependences to those observed is that of shocks at the inner disk and oscillation of the shock position (Molteni et al. 1996; Manickam & Chakrabarti 1999), but there have been objections that such shocks cannot be generated. The correlations between duration of the dips in GRS 1915+105 with the frequency of the QPO are difficult to distinguish from the correlations expected in a viscous refilling model (Trudolyubov et al. 2000).

Finally, Tagger & Pellat (1999) make a case that Rossby waves of the Accretion Injection Instability are a natural way to carry gas and energy from a disk to the corona and thence into a wind or jet and to generate oscillations in the flux.

The data available so far has enough detail to provide many guideposts and constraints to the theories. These low frequency disk-corona oscillations are very common in BHCs and are a challenging physics problem which involves important aspects of accretion onto black holes.

References

Belloni, T., Migliari, S. & Fender, R. P. Disk Mass Accretion Rate and Infrared Flares in GRS 1915+105. In *A&A*, 358:L29, 2000.

Chakrabarti, S.K & Manickham, S. G. XTE J1859+226. In *MNRAS*, 531, L41, 2000.

Chen, X., Taam, R. E. & Swank, J. H. Horizontal Branch Oscillations from Black Hole Candidates. In C. Dermer, M. Strickman & J. Kurfess, editors, *Proceedings of the Fourth Compton Symposium*, AIP, New York, 410:995, 1997.

Cui, W., Zhang, S. N., Focke, W., & Swank, J. H. Temporal Properties of Cygnus X-1 during the Spectral Transitions. In *ApJ*, 484, 383, 1997.

Cui, W., Zhang, S. N., Chen, W., & Morgan, E. H. Strong Aperiodic X-Ray Variability and Quasi-Periodic Oscillationin X-Ray Nova XTE J1550-564. In *ApJ*, 512, L43, 1999.

Dieters, S. W. et al. The Timing Evolution of 4U 1630-47 during Its 1998 Outburst. In *ApJ*, 538:307, 2000.

Hjellming, R. M., Rupen, M. P. & Mioduszewski, A. J. The Radio Counterparts of X-ray Transients Discovered by *RXTE*. In Conference *Rossi*2000, March, 2000.

Markwardt, C. B., Swank, J. H. & Taam, R. E. Variable-Frequency Quasi-Periodic Oscillations from the Galactic Microquasar GRS 1915+105. In *ApJ*, 513:L37, 1999.

Markwardt, C. B., Marshall, F. E. & Swank, J. H. XTE J1859+226. In *IAUC*, 7274, 1999.

Merloni, A., Fabian, A. C. & Ross, R. R. On the interpretation of the multicolour disc model for black hole candidates. In *MNRAS*, 313:193, 2000.

Miyamoto, S., Kimura, K., Kitamoto, S., Dotani, T. & Ebisawa, K. X-Ray Variability of GX 339–4 in its Very High State. In *ApJ*, 383:784, 1991.

Molteni, D., Sponholz, H. & Chakrabarti, S. K. Resonance Oscillation of Radiative Shock Waves in Accretion Disks around Compact Objects. In *ApJ*, 457:805, 1996.

Morgan, E. H., Remillard, R. A. & Greiner, J. *RXTE* Observations of QPOs in the Black Hole Candidate GRS 1915+105. In *ApJ*, 482:993, 1997.

Muno, M. P., Morgan, E. H. & Remillard, R. A. Quasi-Periodic Oscillations and Spectral States in GRS 1915+105. In *ApJ*, 527:321, 1999.

Psaltis, D., Belloni, T. & van der Klis, M. Correlations in Quasi-Periodic Oscillation and Noise Frequencies among Neutron Star and Black Hole X-Ray Binaries. In *ApJ*, 520:262, 1999.

Psaltis, D. & Norman, C. On the Origin of Quasi-Periodic Oscillations and Broad-band Noise in Accreting Neutron Stars and Black Holes. In *ApJ*, submitted 1999 (astro-ph/0001391).

Remillard, R. A., Morgan, E. H., McClintock, J. E., Bailyn, C. D. & Orosz, J. A. *RXTE* Observations of 0.1-300 Hz Quasi-Periodic Oscillations in the Microquasar GRO J1655–40. In *ApJ*, 522:397, 1999.

Rodriguez, J., Varniere, P., Tagger, M. & Durouchoux, Ph. Accretion-Ejection Instability and QPO in Black Hole Binaries: II. Observations. In *A&A*, submitted.

Smith, D. M., Heindl, W. A., Swank, J., Leventhal, M., Mirabel, I. F. & Rodriguez, L. F. X-Ray Timing in 1E 1740.7-2942 and GRS 1758-258. In *ApJ*, 489:L51, 1997.

Sobczak, G. J., McClintock, J. E., Remillard, R. A., Cui, W., Levine, A. M., Morgan, E. H., Orosz, J. A., Bailyn, C. D. Correlations between Low-Frequency Quasi-periodic Oscillations and Spectral Parameters in XTE J1550-564 and GRO J1655-40. In *ApJ*, 531:537, 2000.

Tagger, M. & Pellat, R. An accretion-ejection instability in magnetized disks . In *A&A*, 349, 1003, 1999.

Takizawa, M. et al. Spectral and Temporal Variability in the X-Ray Flux of GS 1124-683, Nova Muscae 1991. In *ApJ*, 489, 272, 1997.

Trudolyubov, S., Churazov, E. & Gilfanov, M. The 1-12 HZ QPOs and dips in GRS 1915+105: tracers of Keplerian and viscous time scales? In *A&A*, 351, L51, 2000.

Wijnands, R. & van der Klis, M. The Broadband Power Spectra of X-Ray Binaries. In *ApJ*, 514, 939, 1999.

RXTE Observations of the New X-ray Transient XTE J1859+226

Craig Markwardt (craigm@lheamail.gsfc.nasa.gov)
University of Maryland, NASA/GSFC

Abstract. We present results of RXTE observations of XTE J1859+226, a transient and probable microquasar discovered in October, 1999. The light curve approximately followed a fast-rise exponential-decay, with a peak flux of about 1.2 Crab (2–10 keV). The source is at a galactic latitude of $+8.5^{\circ}$, which makes it difficult to estimate distance and luminosity precisely. QPOs were detected in the 150–200 Hz and 0.5–10 Hz ranges. The high frequency QPOs and the results of spectral fitting can be used to loosely constrain the central object mass.

Keywords: microquasar, black hole, XTE J1859+226, QPO

1. Introduction

Microquasars, as originally embodied in the prototype object GRS 1915+105, are probable stellar-mass black holes with relativistic jet outflows (Mirabel & Rodriguez 1998). Since the discovery of GRS 1915+105, it seems that microquasars may be ubiquitous. Here we present RXTE X-ray observations of the new transient XTE J1859+226, which may indeed be another microquasar.

The galactic source XTE J1859+226 was discovered as an X-ray transient by the RXTE All-Sky Monitor in October 1999 (Wood et al. 1999). RXTE observations were initiated and continued for several subsequent months. The X-ray light curve bears some resemblance to the well-known fast-rise exponential-decay profile (Figure 1), with a rise time to peak of a few days, followed by a somewhat chaotic X-ray plateau lasting a few weeks, and then a gradual decline over several hundred days. The decline phase contained a secondary plateau ~ 60 days after maximum.

The peak flux was achieved on October 16 at a level of 5×10^{-8} erg s^{-1} cm^{-2} in the 2–80 keV band, which corresponds to a luminosity of 6×10^{38} d_{10}^{2} erg s^{-1} where d_{10} is the distance in units of 10 kpc. Spectrally, the source began its rise in a very hard state, softened as it peaked in intensity, and continued to soften in its decline. This evolution is remarkably similar to that of GRS 1915+105 in its low-hard state, and the transient outburst of 4U 1630–47, another soft X-ray transient and black hole candidate (Dieters et al. 2000).

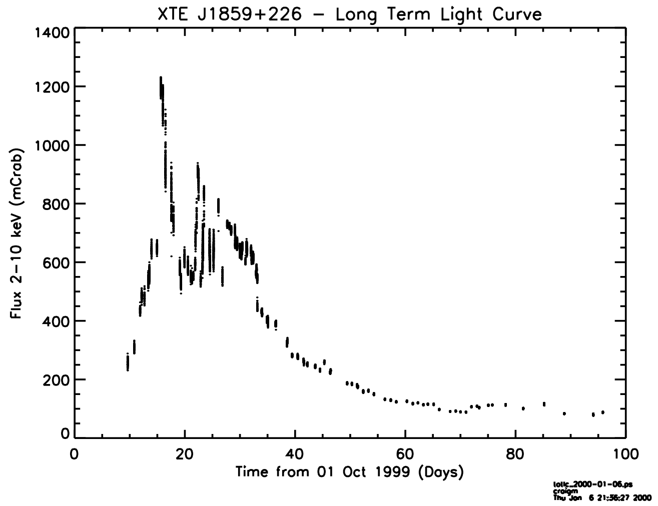

Figure 1. RXTE PCA light light curve of the October, 1999, outburst of XTE J1859+226 (2–10 keV).

Extensive optical and radio monitoring also took place (summarized by Hjellming at `http://www.aoc.nrao.edu/~rhjellmi/x1859.html`). The observations suggest at least two relativistic ejection episodes occurred over the course of the plateau phase: two flares occurred on approximately October 16.5 and 27, with subsequent power law declines and progressive spectral steepening. This evolution is indeed reminiscent of the expansion of a relativistic fireball, as first advanced Mirabel et al. (1998) for GRS 1915+105. In the case of XTE J1859+226, no actual ejecta were spatially resolved.

Continued optical and RXTE PCA observations of the source as it passed into quiescence have revealed low level activity in the summer of 2000 (Casares et al. 2000; Tomsick & Heindl 2000). Optical modulations have been detected at several periods, with the consensus settling on a multiple of 9.1 hr (eg., Sanchez-Fernandez et al. 2000).

The source is located at galactic latitude $+8.5°$. Optical extinction measurements of $E(B-V) = 0.8 \pm 0.4$ (Wagner et al. 1999) and 0.58 ± 0.07 (Hynes et al. 1999) suggest a minimum distance of a 1–3 kpc, which is consistent with the fitted value of neutral hydrogen absorption in the PCA/HEXTE spectrum, $N_H = 1.1 \times 10^{22}\,\mathrm{cm}^{-2}$. However, as the source is out of the galactic plane it is difficult to place an upper limit to the distance.

2. Fourier and Energy Spectra

Both high and low frequency quasiperiodic oscillations have been detected in the X-ray light curves of the source (Cui et al. 2000; Markwardt et al. 2000). In an average of the highest intensity power spectra, we find a broad high frequency QPO with a centroid frequency of 175 Hz and a full-width half-maximum of 120 Hz. Such high frequency oscillations have been seen in a number of black hole candidates (in the range 67–300 Hz) and at very least suggest they derive from phenomena close to the black hole horizon. Even when a distinct peak is not visible, the harder observations contain a broadband noise component which extends detectably to at least 250 Hz. Cui et al. (2000) report marginally distinct QPO frequencies of 187 ± 14 Hz and 150 ± 28 Hz. These features suggest that the QPO centroid frequency is variable, but reaches a maximum frequency of 200–300 Hz, as might be expected if the oscillation reached an inner boundary such as the innermost radius of stable orbits.

Lower frequency QPOs were detected intermittently throughout the outburst in the approximate range of 0.5–10 Hz. Often triplet peaks were observed, having the ratio of centroid frequencies of 1–2–4. As the center peak was usually the strongest, this arrangement strongly implies a subharmonic relationship. Such subharmonics have been seen recently in another black hole candidate XTE J1550–564 (Sobczak et al. 2000). Both low and high frequency QPOs have been seen simultaneously.

Energy spectra were generated from the combined PCA and HEXTE observations, and satisfactorily fitted by a model consisting of a multicolor disk and a power law with Compton reflection. During the plateau the inner disk temperature was typically 0.85 keV but the power law component dominated (photon index $\sim$2.5). Around November 5 the disk component became dominant, and the source began its slow decline in temperature and intensity.

The inner radius of the disk may be estimated from the X-ray flux and temperature, and also considering the color correction factor X that takes into account X-ray scattering and inclination effects (Zhang, Cui & Chen 1997). Using a value of $X \sim 3$, we arrive at $R_{\rm in} \simeq 80 - 100$ km d_{10}, based on a reasonable range in minimum X-ray fluxes during the plateau phase. The mass and radius can also be constrained by considering that the maximum frequency observed, 200–250 Hz is bounded by the frequency at the radius of marginally stable circular orbits. Using these limits, we derive the approximate mass limit $M < 11 M_{\odot}$, and the distance lies in the range 5–13 kpc. For a maximally rotating black hole, $M < 30M_{\odot}$. The main uncertainties lie in the distance to the source and the color correction factor.

There may be a weak disk-jet connection in this source. Of the two radio/IR ejection events, the first on October 16.5 involved the temporary disappearance of the low frequency QPO, and the second on October 27 involved the disappearance of both low and high frequency QPOs (the high frequency QPO did not resume subsequently). While there were no particularly strong drops in the disk flux (which might be tied to the loss of the inner accretion disk, as in GRS 1915+105), the disappearances of the QPOs suggests that there may indeed have been some mild disruptions in the inner accretion disk dynamics caused by the ejection events.

This work was produced in collaboration with Warren Focke and Jean Swank. I also thank Rob Hynes and Tariq Shahbaz for useful discussions during the Workshop.

References

Casares, J. et al. "XTE J1859+226." IAUC No. 7451, 2000.

Cui, W., Shrader, C. R., Haswell, C. A., & Hynes, R. I. Discovery of High-Frequency Quasi-periodic Oscillations in the Black Hole Candidate XTE J1859+226. ApJ, 535:L123-127, 2000.

Dieters, S. W., et al. The Timing Evolution of 4U 1630–47 During Its 1998 Outburst. ApJ, 538:307–314, 2000.

Hynes, R. I., Haswell, C. A., Norton, A. J., Chaty, S. "XTE J1859+226." IAUC No. 7294, 1999

Markwardt, C. B., Focke, W. B., Swank, J. H., & Taam, R. E. RXTE Variability Study of the New X-ray Transient XTE J1859+226. BAAS, 31(5): 1555, No. 126.03, 1999.

Mirabel, I. F., et al. Accretion Instabilities and Jet Formation in GRS 1915+105. A&A, 330:L9–L12, 1998.

Mirabel, I. F. & Rodríguez, L. F. Microquasars in our Galaxy. Nature, 392: 673–676, 1998.

Sanchez-Fernandez, C., Zurita, C., Casares, J., Shahbaz, T., Castro-Tirado, A. "J1859+226." IAUC No. 7506, 2000.

Sobczak, G. J., Remillard, R. A., Muno, M. P., McClintock, J. E. Characterizing the Low-Frequency QPO Behavior of the X-ray Nova XTE J1550–564. ApJ, in press (astro-ph/0004215).

Tomsick, J. A., & Heindl, W. A. "XTE J1859+226." IAUC No. 7456, 2000.

Wagner, R. M., Smith, P. S., Schmidt, G. D., & Shrader, C. R. "XTE J1859+226." IAUC No. 7279, 1999.

Wood, A., Smith, D. A., Marshall, F. E., Swank, J. "XTE J1859+226." IAUC No. 7274, 1999.

Zhang, S. N., Cui, W., & Chen, W. Black Hole Spin in X-Ray Binaries: Observational Consequences. ApJ, 482:L155–L158, 1997.

XTE J1118+480: Clues on the Nature of the Accretion Flow from the Optical Variability

A. Merloni[1], T. Di Matteo[2]* and A. C. Fabian[1]
1 *Institute of Astronomy, Madingley Road, Cambridge, CB3 0HA, UK*
2 *Harvard-Smithsonian Center for Astrophysics, 60 Golden St., Cambridge, MA 02138, USA*

Abstract. We show how the simultaneous presence of a strong quasi periodic oscillation (QPO) of period $\sim$10 seconds in the optical and X-ray lightcurves of the X-ray transient XTE J1118+480 can be used to obtain information about the nature of the accretion flow around the source. The unusually high optical-to-X-ray flux ratio and the QPO observed simultaneously in both energy bands suggest that a significant fraction of the optical flux might originate close to the central source, where most of the X-rays are produced and be indicative of a magnetically dominated corona. We also show how the temporal evolution of the QPO can provide us with information on both the inner radius and the viscous properties of the optically thick accretion disc.

Keywords: accretion disk, magnetic field, XTE J1118+480

1. Introduction: The Magnetic Corona Model

The transient X-ray source XTE J1118+480 was discovered with the RXTE All-Sky Monitor on March 29, 2000 (Remillard et al. 2000). At the peak of its outburst, it showed an X-ray spectrum typical of black hole candidates (BHC) in their *hard* state, with a prominent power-law component (photon index of about 1.8). The 13th magnitude optical counterpart, discovered by Uemura, Kato & Yamaoka (2000), exhibited a spectrum fairly typical of X-ray Novae in outburst (Dubus et al. 2000 and references therein). A strong QPO with frequency $\nu_{\rm QPO} \sim 0.1$ Hz has been found in the X-ray power density spectrum (PDS) of the source (Wood et al. 2000); more surprisingly, the optical lightcurves also showed a prominent QPO at the same frequency (Haswell et al. 2000). The QPO frequency drifted to higher values systematically in both bands for about two months.

As discussed in detail in Merloni, Di Metteo & Fabian (2000) (MDF), the high optical-to-X-ray flux ratio and the optical/UV variability argues for the presence of significant cyclo-synchrotron (CS) radiation from active regions in a magnetically dominated corona in this source. Assuming that a fraction of the observed optical flux corresponding to

* Chandra fellow

its oscillating part ($\sim 30\%$) is due to CS emission from a magnetized corona, we modeled the spectrum taking into account reprocessing of coronal radiation in the accretion disc (according to the height of the active regions) and all the relevant radiative processes (see MDF for details). The disc was assumed to extend down to the innermost stable orbit of a non-rotating black hole ($R_{\rm in} = 6GM/c^2 = 3R_{\rm S}$). We found that, in order to match the high (compared to X-rays) optical flux, both a low accretion rate ($\dot{M}/\dot{M}_{\rm Edd} = \dot{m} \simeq 0.01$), and a high fraction of accretion power dissipated in the corona ($f > 0.9$) are needed; also the active regions need to be high above the disc (at about $10R_{\rm S}$)[1].

Hynes et al. (2000) reporting on *EUVE* observations of the source showed that the low measured EUV flux is inconsistent with an optically thick disc extending down to radii $R < 1000R_{\rm S}$ (but see Dubus et al. 2000 for a different estimate of the EUV flux). Based on this, they favor an inner advection-dominated flow (ADAF) surrounded by a geometrically thin disc truncated at hundreds of $R_{\rm S}$. In the next section we show how to use the variability information to put constraints on the inner disc location.

2. The QPO Viscous Evolution

Beside the peaked QPO around 0.1 Hz, the observed PDS of XTE J1118+480 exhibits a broader feature around 1 Hz; plotted one against the other, these frequencies fall remarkably well on the correlation among QPOs discovered by Psaltis, Belloni & van der Klis (1999) in the PDS of BHC and neutron stars. Such a correlation is likely to reflect a general property of the accretion flows around these objects. Here we assume that the QPO observed in XTE J1118+480 is produced at a specific distance ($R_{\rm t} = r_{\rm t} R_{\rm S}$) where a discontinuity of the flow occurs, as in Psaltis & Norman (2000). The QPO frequency must be essentially determined by the relativistic dynamical frequencies of the system (Psaltis & Norman 2000; Stella, Vietri & Morsink 1999).

XTE J1118+480 observations offer the opportunity to track the QPO evolution over a long period of time (Wood et al. 2000). To model such evolution, we calculate $R_{\rm t}(t)$ integrating the equation of the viscous evolution of a standard Shakura-Sunyaev disc:

$$\frac{\partial R_{\rm t}}{\partial t} = -\frac{3}{2}\alpha \left(\frac{H}{R_{\rm t}}\right)^2 \left(\frac{GM}{R_{\rm t}^3}\right)^{1/2} J^{-1}, \qquad (1)$$

[1] Alternatively, a good agreement with the data could be achieved if the active regions move relativistically away from the disc (MDF, see also Markoff, Falcke & Fender 2000 for a jet model of the SED)

(a) $\nu_{\rm QPO}$=2$\nu_{\rm LT}$; rad. p.; χ^2/dof=0.21; $\alpha[\dot{m}(1-f)]^2 \simeq 4.5 \times 10^{-8} a^{7/6} m^{-1/6}$ | (b) $\nu_{\rm QPO}$=$\nu_{\rm Kep}$; gas p.; χ^2/dof=0.80; $\alpha^{4/5}[\dot{m}^2(1-f)]^{1/5} \simeq 2.5 \times 10^{-4} m^{4/15}$

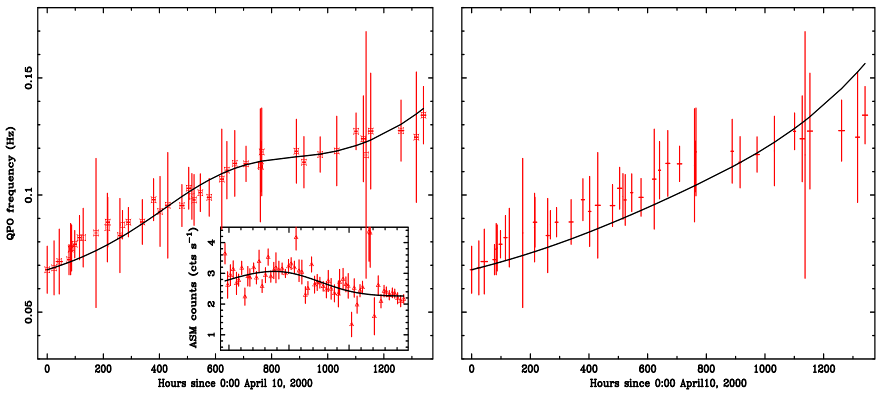

Figure 1. Fit to the observed QPO evolution (RXTE and USA data, Wood et al 2000) for (a) a QPO produced by relativistic LT precession in a radiation pressure dominated disc and (b) a QPO produced by modulation with Keplerian frequency in a gas pressure dominated disc. The error bars are given by the QPO FWHM, which is likely to reflect the uncertainties in the location where the oscillation are excited. In the inset the ASM lightcurve of XTE J1118+480 (triangles): the continuous line is a SPLINE fit to its smooth variation (flares are excluded), which is assumed to reflect long term variations of the total accretion rate.

where J=$1-\sqrt{3/r_{\rm t}}$, α is the viscous parameter and the disc scaleheight $H/R_{\rm t} \simeq 9\dot{m}J(1-f)r_{\rm t}^{-1}$ for a radiation pressure dominated disc and $H/R_{\rm t} \simeq 0.02(\alpha m)^{-1/10}(\dot{m}J)^{-1/5}(1-f)^{-1/10}r_{\rm t}^{1/20}$ for a gas pressure dominated one (Merloni, Fabian & Ross 2000). We test two different hypothesis on the origin of the QPO (and the accretion flow geometry):

(a) According to the relativistic precession interpretation of the observed correlation (obeyed by XTE J1118+480) $\nu_{\rm QPO}$ is twice the nodal precession frequency: $\nu_{\rm QPO}$=$2\nu_{\rm nod} \simeq 1.62 \times 10^4 (a/m) r_{\rm t}^{-3}$ Hz, implying $r_{\rm t} \sim 50(a/m)^{1/3}$ (a is the BH angular momentum, m its mass in Solar mass units). In this case the radiation pressure solution, appropriate for the inner part of an optically thick disc, should be used in Eq (1).

(b) Alternatively, the observed low frequency QPO can be due to a Keplerian modulation of the flow: $\nu_{\rm QPO}$=$\nu_{\rm Kep} \simeq 1.14 \times 10^4 m^{-1} r_{\rm t}^{-3/2}$ Hz, so that $r_{\rm t} \sim 2000\, m^{-2/3}$, and the gas pressure solution must be used in this case.

Furthermore, we assume that the smooth variations of the X-ray ASM luminosity reflects a modulation of the total accretion rate so that $\dot{m}(t)$=$g(t)\dot{m}_0$, where $g(t)$ is the continuous function shown in the inset in Fig. 1. We integrate Eq. (1) and fitted the temporal evolution of the QPO frequency with the resulting $\nu_{\rm QPO}(R_{\rm t}(t))$ for the two cases and show the results in Fig. 1. Both fits are acceptable, but the relativistic precession model (with $r_{\rm t}$=$O(10)$) explains the QPO evolution better than the Keplerian one (with $r_{\rm t}$=$O(1000)$). Finally, from such fits we can obtain an estimate of the viscous parameters of the optically thick accretion disc (α, $\dot{m}$, f, through the products shown in Fig. 1) independent on any spectral analysis. The estimate from MDF ($\dot{m}f \simeq 10^{-3}$) based on the magnetic corona model is also consistent with case (a) (with $\alpha \sim 0.01$), while for case (b) it would imply an unreasonably low viscosity.

3. Conclusions

The main rationale for our model is the simultaneous presence of a strong QPO in the optical and X-ray lightcurves of XTE J1118+480, suggesting that the fluxes in the two bands both originate from the same region in the inner part of the accretion flow. Self-absorbed CS emission is the natural candidate to explain the optical variability. Such emission is expected in any magnetic corona model, and the inferred magnetic field value ($B \approx 2 \times 10^6$ G) is the one predicted to arise when the source is in the *hard* state (MDF). We have also shown how the evolution of the QPO can be satisfactory accounted for if the QPO is produced by a modulation whose frequency is equal to twice the relativistic nodal precession in a radiation pressure dominated disc and the location of such modulation (that is perhaps where the inner accretion disc undergoes a transition and is *at most* a few tens of Schwarzschild radii) viscously drift inwards.

References

Dubus, G. et al., 2000, submitted to ApJ (astro-ph/0009148)
Haswell et al., 2000, IAUC 7427
Hynes, R. I. et al., 2000, ApJ, 539, L37
Markoff, S., Falcke, H. & Fender, R. P., 2000, submitted to ApJ
Merloni, A., Di Matteo, T. & Fabian, A., 2000, MNRAS, 318, L15 (MDF)
Merloni, A., Fabian, A. C. & Ross, R. R. 2000, MNRAS, 313, 193
Psaltis, D., Belloni, T. & van der Klis, M., 1999, ApJ, 520, 262
Psaltis, D. & Norman, C., 2000, ApJ in press (astro-ph/0001391)
Stella,L., Vietri, M. & Morsink, S., 1999, ApJ, 624, L63
Remillard, R. R., et al., 2000, IAUC 7390
Uemura, M., Kato, T. & Yamaoka, H., 2000, IAUC 7390
Wood, K. S. et al., 2000, ApJL in press (astro-ph/0006234)

Comptonization and Phase Lag Correlations in GRS 1915+105

L. Nobili[1], T.Belloni[2] , R. Turolla[1] and L. Zampieri[1]
[1]*Dipartimento di Fisica "G.Galilei", Università di Padova (Italy)*
[2]*Osservatorio Astronomico di Brera, Merate (Italy)*

Abstract. We suggest a simple thermal Comptonization model to account for the observed phase lags-hardness ratio correlation of GRS1915+105.

Keywords: accretion, accretion disk, GRS 1915+105

Some distinctive features make GRS 1915+105 atypical with respect to Galactic BHCs (Belloni et al., 2000 and reference therein). The dramatic drop in luminosity seen at certain stages and the simultaneous hardening of the spectrum plays in favor of the onset of an instability that in a very short time disrupts the inner part of the disk. This hypothesis is partially supported by theoretical calculations in which a thermal-viscous instability blows off the inner, radiation-pressure supported region of the disk (Szuszkiewicz and Miller, 1998). This event marks the transition from the so called high/soft state B, characterized in large part by a multi–temperature black body emission from a standard disk (high count rate in the soft X–ray band), to a low/hard state C, in which the primary emission is presumably due to a semi-evacuated disk lacking of its most luminous inner region. A relevant feature displayed by GRS 1915+105 during state C is the tight correlation between the 0.5–8 Hz QPO and the spectral and variability properties (Reig et al., 2000). However, while a number of properties are easily interpreted in terms of the disk refilling model, the presence of time lags between hard and soft photons is not well understood yet. Even more intriguing is the observed gradual decrease of the time–lags from positive to negative values during the late state C. Because of this unusual behaviour, it is conceivable that the working mechanism could be slightly different from that usually assumed in other Galactic X–ray binary system. In fact, models based on a disk surrounded by a hot comptonizing corona cannot explain the timing properties of GRS 1915+105 and always produce positive lags.

To overcome these difficulties, we suggest here a different scenario for the accretion flow in the central region of GRS 1915+105, still within the framework of thermal Comptonization. The starting point is based on the following considerations: *i)* the strong correlations among the relevant spectral and timing properties of the source and their nearly regular evolution imply that a unique mechanism (i.e. the comptonizing cloud) is at work for the entire duration of state C. Then the continuous variation of the physical parameters of the cloud modulate the emerging flux. *ii)* The regular transition from positive to negative lags requires that the relative temperature of the cloud and the incident photons changes in time, starting from a value which is initially higher than the incident mean photon temperature T_γ, evolving to lower values at later time.

Taking into account these two basic facts, we have assumed that during state C a cloud formed e.g. by the debris of the puffed-up inner region or by the evaporation of the disk itself, fills the central region of the configuration. During the replenishment of the semi–evacuated part of the disk the cloud, assumed not uniform in temperature, becomes more and more compact, following the inward motion of the disk edge.

Since the cloud shrouds the inner part of the disk, in absence of an efficient heating mechanism electrons should be quickly cooled down by soft photons. However, if cooling of ions is inefficient, like in advection–dominated flows, protons decouple from electrons and reach a temperature that is a fraction $\eta \lesssim 1$ of the virial temperature, $KT_i \approx \eta G M m_p/r$. The electron thermal balance will be then fixed by the competition between ion heating and Compton cooling. A simple computation shows that, even if not complete virial equilibrium is achieved, the electron temperature T_H of the inner part of the cloud can be as high as 10 keV or more, depending weakly on the location of the inner edge of the disk, r_{in}. Moreover, the temperature $T(r)$ is one order of magnitude smaller at greater distance (see for details Nobili et al.,2000). Since our aim is simply to test the capability of the model to reproduce the correct trend of the evolution and to estimate the amplitude of the spectral variations of GRS 1915+105, we have approximated the temperature stratification by assuming that the cloud is formed by an inner hot sphere at uniform temperature $T_H \approx 15$ keV, and an external cold shell at temperature $T_W \approx 1.5$ keV. The scattering depths of these two regions are τ_W and $\tau_H > \tau_W$ respectively. Initially the cloud is extended and rarefied so that soft photons are preferentially scattered in the inner and very hot part, where $\tau_H \gtrsim 1$, while the cold external shell does not play any role since $\tau_W \ll 1$ there. Under such conditions radiation gains energy producing a positive lag.

As density increases, the Compton y-parameter of the corona increases, until it exceeds unity below a certain radius r_{sc}. Photons emitted by the inner part of the disk undergo repeated scatterings with the hot electrons and start to fill the Wien peak at T_H. Then the primary radiation is formed by the flux emitted by the disk plus the hot, dense part of the corona. The resulting spectrum is therefore the superposition of a multitemperature blackbody (BB) generated by the disk at $r > r_{sc}$, and a Bose-Einstein distribution at T_H (BE). Both components contribute to the total spectrum in a variable way, depending on the extension of the region between r_{sc} and the disk inner edge r_{in}. In particular, for $r_{in} > r_{sc}$ (i.e. the Compton parameter is below 1 everywhere) the initial photon occupation number n is that of a pure multitemperature blackbody of a disk truncated at r_{in}. However, when $r_{in} < r_{sc}$ the BB+BE radiation has to traverse the warm part of the corona before escaping to infinity. In doing so, photons are downscattered producing now a negative lag.

The theoretical calculation of the emerging spectrum proceeds in two steps. First, we compute the time-dependent comptonized spectrum for a given seed photon distribution by solving the Kompaneets equation in a semi-infinite homogeneous medium and then we use an escape probability algorithm to obtain the time evolution of the spectrum emerging from a medium of finite depth.

The results presented here have been obtained for $T_H = 15$ keV, $T_W = 1.5$ keV, $r_{sc} = 20$ and a black hole mass $M = 6M_\odot$. The model with $r_{in} = 16$ (in units of GM/c^2) corresponds to the usual picture in which a hot corona ($T = T_H$) of moderate depth ($\tau = \tau_H \sim 3$) upscatters the soft photons produced by the disk; under these conditions the energy exchange in the warm region can be reasonably assumed to be negligible. The opposite situation is represented by the model with $r_{in} = 6$. Now the disk inner region lies entirely within the hot part of the corona which, because of the increase in the density, has $\tau_H \gtrsim 100$. Escaping photons are then reprocessed in the outer, warm part of the corona ($T = T_W$, $\tau = \tau_W \sim 10$).

The comparison of our results with observational data is illustrated in Figure 1. Panel 1a shows the color-color evolution, with colors defined as the ratios HR1=(5-13 keV)/(2-5 keV) and HR2=(13-60 keV)/(2-5 keV). The observed hardness ratios are quite well reproduced by the model for a value of the column density $N_H = 2 \times 10^{22}$ cm^{-2}, consistent with observations (Belloni et al. 2000). When the inner edge of the disk is far out, the spectrum is a power-law produced by thermal Comptonization of soft disk photons. As r_{in} decreases, downscattering becomes progressively more important with respect to upscattering in the hot corona, the spectrum softens and, at the same time, the phase lag of the continuum decreases. Eventually, systematic downscattering dominates and soft 2–5 keV photons, which underwent more scatterings, escape later than hard 5–13 keV photons, *causing an inversion in the sign of the lag*. Panels 1b and 1c show the lag of the continuum as a function of the color HR1=(5-13 keV)/(2-5 keV) and QPO frequency (the scattering of the computed points is partially due to the poor sampling of the parameter space). Time lags have been

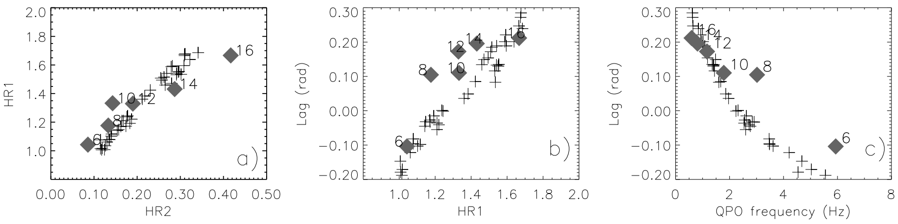

Figure 1. Comparison between observed data (plus sign) and calculated values (filled diamonds). a) color-color diagram; b) phase lags of the continuum versus HR1; c) phase lags versus QPO frequency. Each model is labeled by the value of r_{in} in units of GM/c^2.

computed assuming that the typical size r_c of the comptonizing cloud is directly correlated with the inner edge of the disk, and varies with time in the range $20 \lesssim r_c c^2/GM \lesssim 400$. Finally, we derived a relation between ν_{QPO} and r_{in} associating the model with $r_{in} = 6$ (16) to the observation with the largest (smallest) QPO frequency, 6 (0.6) Hz. This yields $r_{in} \approx 13\nu_{QPO}^{-0.43}$. It is interesting to note that this relation is similar to that found in a quite independent way by di Matteo & Psaltis (1999) combining an empirical relation with the upper bound provided by the Keplerian orbital frequency.

Ultimately, despite the drastic simplification introduced in our calculations, a simple Compton model can account for the main observational properties of GRS 1915+105 in state C. In particular, we have adopted here an *ad hoc* picture for the accretion flow, but the basic results are largely independent of the specific choice for the geometry. Within a Comptonization framework the main ingredients to account for the observed correlations are the presence of a non isothermal cloud of varying optical depth and a source of energetic primary photons at small radii. However, we must consider also the possibility that dynamical Comptonization, due e.g. by a not uniformly expanding cloud or jet, could play a relevant role in producing the observed phenomenology.

References

Belloni,T. et al. A model-independent analysis of the variability of GRS 1915+105. *Astron.Astrophys*, 355: 271-290, 2000

di Matteo, T. and Psaltis, D., Quasi-Periodic Variability and the Inner Radii of Accretion Disks in Galactic Black Hole Systems. *ApJ*, 526: L101-L104, 1999

Nobili,L., Turolla,R., Zampieri,L. and Belloni,T., A Comptonization Model for Phase Lag Variability in GRS 1915+105 *ApJ*, 538: L137-L140, 2000

Reig, P., et al., Phase Lag Variability Associated with the 0.5-10 HZ Quasi-Periodic Oscillations in GRS 1915+105. *ApJ*, 541: 883-888, 2000

Szuszkiewicz, E. and Miller, J.C., Limit-Cycle Behaviour of Thermally Unstable Accretion Flows on to Black Holes. *MNRAS*, 298: 888-896, 1998

X-ray flares/bursts from GRS 1915+105 and the two component accretion flow

J.S. Yadav* and A.R. Rao
Tata Institute of Fundamental Research, Homi Bhabha Road, Mumbai, 400 005, India

Abstract. We present results of our analysis of a set of RXTE/PCA observations of X-ray flares/bursts with burst cycle ranging from 30 to 1300 s from the Galactic X-ray transient source GRS 1915+105 during last four years. These flares/bursts can be classified into four types: 1) regular bursts with short burst phase of $\sim$ 20 s (R1), 2) regular bursts with short quiescent phase of $\sim$ 20 s (R2), 3) long regular bursts (R3) with burst cycle $\geq$ 1000 s, and 4) irregular bursts (IR). For all the observed bursts, the duration of the quiescent phase is inversely proportional to the square of the QPO frequency (2−10 Hz).

Keywords: accretion, black hole, GRS 1915+105

1. Introduction

The Galactic X-ray transient source GRS 1915+105 has shown spectacular X-ray variability during last four years of its observation by RXTE and other satellites (Greiner et al., 1996, Yadav et al., 1999, Belloni et al., 2000). This source was discovered in 1992 with the WATCH all sky X-ray monitor onboard the GRANAT satellite (Castro-Tirado et al. 1994). The X-ray intensity was found to vary on a variety of time scales and the light curve showed a complicated pattern of dips and rapid transitions between high and low intensity (Belloni et al., 1997, Taam et al., 1997). Recently, Yadav et al. (1999) have made a detailed study of various types of X-ray bursts seen in GRS 1915+105 from IXAE/PPCs observations during 1997 June - August and attempted to explain these bursts in the light of the recent theories of advective accretion disks. In X-ray astronomy, the terminology X-ray burst is used for type I and type II classical bursts seen in LMXBs. The timing and spectral properties of the flares/bursts described here are completely different than that of the classical bursts (Yadav & Rao, 2000).

In Table 1, we list details of RXTE/PCA observations discussed here along with some of the properties of the observed X-ray flares/bursts. Each burst cycle consists of a low flux quiescent phase followed by a high flux burst phase and the fast transition in less than 10 s. The

* Email: jsyadav@tifr.res.in

Table I. Summary of selected observations of GRS 1915+105

Date (UT)	Exposure (s)	Type of Bursts	ASM[a] Flux	Rec. Time (s)	Av. Q. Flux
1996 April 06 05:40	5600	Regular (R2)	99.4	280[b]	6200
1996 Oct 07 05:44	7000	Regular (R3)	98.8	1150[b]	3200
1997 May 26 12:25	3215	Regular (R1b)	47.6	105[b]	7500
1997 June 18 14:17	3472	Irregular (IR)	61.5	var.	var.
1997 June 22 19:27	2550	Regular (R1a)	59.7	55[b]	8700

Q. Flux= average quiescent time flux (c/s), var. = variable, [a]Mean ASM flux (c/s) for a day, [b]Mean burst recurrence time.

dips or the quiescent phase in these observations are spectrally hard while the brighter portions (the burst phase) are soft (Yadav, 2000). For details of these observations as well as of our analysis please see Yadav & Rao (2000).

2. Results and Discussion

On the basis of timing properties, these flares/bursts can broadly be put into two classes: regular bursts centered around a fixed period with low dispersion ($\delta P/P \sim 1-50\%$) and irregular bursts with no fixed periodicity ($\delta P/P > 50\%$). These flares/bursts can be classified into four types: 1) regular bursts with short burst phase of $\sim$ 20 s (R1) with $\delta P/P \sim$ 1-10%, 2) regular bursts with short quiescent phase of $\sim$ 20 s (R2) with $\delta P/P$ up to 50%, 3) long regular bursts (R3) with burst cycle $\geq$ 1000 s and $\delta P/P \sim 1{-}15\%$, and 4) irregular bursts (IR) (see Fig. 1). We have measured the quiescent time and the burst duration for all types of bursts and results are shown in Fig. 1. The data of IR bursts seen on 1997 June 18 fall diagonally; clearly showing a strong correlation between the burst duration and the quiescent time. On the other hand, data for different types of regular bursts fall on either horizontal or vertical branches implying no such correlation for the regular bursts (Yadav et al., 1999). The R1a and R1b regular bursts fall on the horizontal branch with the burst time $\sim$ 20 s. The R2 regular bursts fall on the vertical branch with the quiescent time $\sim$ 20 s while the R3 regular bursts fall on vertical branch with the quiescent time $\sim$ 320 s (this is shown in the inset of Fig. 1).

The most striking features of these flares/bursts are slow exponential rise, sharp linear decay and hardening of spectrum as burst progresses (Paul et al. 1998). The decay time scales are shorter than the rise time

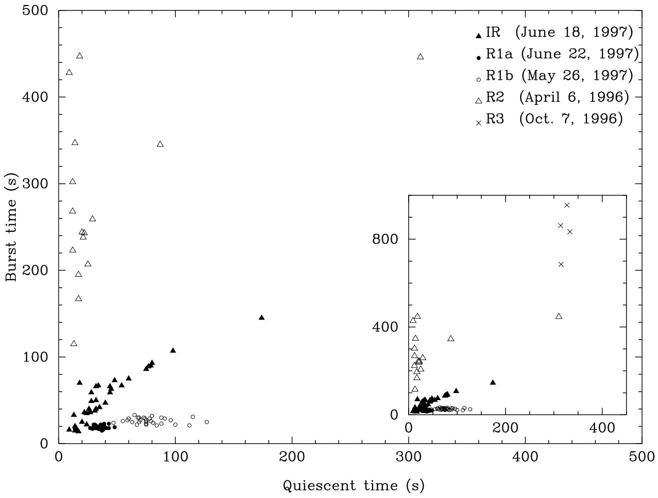

Figure 1. Plot of the quiescent time and the burst duration for all the bursts.

scales. In sharp contrast, the decay time is longer than the rise time in classical bursts and spectrum is initially hard and becomes softer as the burst decays (Lewin et al., 1995). Yadav et al. (1999) have suggested that the source is in a high-soft state during the burst phase and in a low-hard state during the quiescent phase on the basis of available spectral observations and derived disk parameters of GRS 1915+105. The fast time scale for the transition of the state is explained by invoking the appearance and disappearance of the advective disk in its viscous time scale. Such fast changes of states are possible in the Two Component Accretion Flows (TCAF) where the advective disk covers the standard thin disk (Chakrabarti, 1996, Chakrabarti and Titarchuk, 1995). Chakrabarti & Manickam (2000) have provided a relation; $t_{off} = f(\Theta_{\dot{M}})\nu_I^{-2}$ based on TCAF. Where t_{off} is the duration of off state (duration in which the sonic sphere becomes ready for catastrophic Compton cooling), ν_I is the intermediate QPO frequency between $2 - 10$ Hz, and $\Theta_{\dot{M}}$ is a dimensionless parameter defined as $\Theta_{\dot{M}} = (\Theta_{out}/\Theta_{in}) \times \dot{m}_d$ where Θ_{in} and Θ_{out} are the solid angles of the inflow & outflow respectively and $\dot{m}_d$ is the disk accretion rate in units of Eddington accretion rate.

In Fig. 2 we plot the above relation in the log - log scale taking t_{off} as the quiescent time for $\Theta_{\dot{M}} = 0.0145$, 0.0245 and 0.0335 alongwith our QPO results (points). These results are in good agreement. The data points of R2 and R3 bursts when ASM flux was 99.4 & 98.8 c/s respectively fall along the dotted line with $\Theta_{\dot{M}} = 0.0335$ (see table 1). The data points of R1a and IR bursts when ASM flux was 59.7 and 61.5 c/s respectively fall along the dashed - dotted line ($\Theta_{\dot{M}} = 0.0245$).

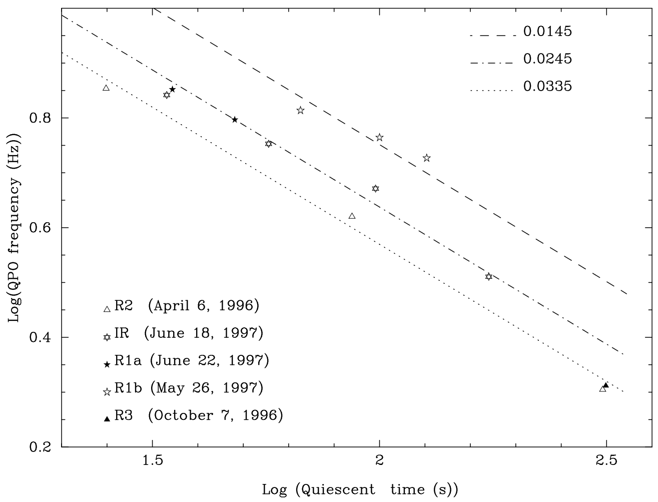

Figure 2. Variation of QPO frequency ν_I (minimum) with the quiescent time for different types of X-ray flares/bursts (data points). Plotted lines are the quiescent time $\alpha\ \nu_I^{-2}$ for different values of $\Theta_{\dot{M}}$.

The data points of R1b bursts during which ASM flux has lowest value of 47.6 c/s fall along the dashed line ($\Theta_{\dot{M}} = 0.0145$). It may be noted here that the $\Theta_{\dot{M}}$ and the ASM flux though determined independently agree well for different types of flares/bursts as both of these are related to the disk accretion rate $\dot{m}_d$. Our results in Fig. 2 suggest that $t_{\rm off}$ represents the quiescent time of the flares/bursts which may or may not be of the order of the viscous time scales of a thin accretion disk.

References

Belloni, T., et al., *ApJ*, **488**, L109, 1997.
Belloni, T., et al., *A & A*, **355**, 271, 2000.
Castro-Tirado, A. J., et al., *ApJS*, **92**, 469, 1994.
Chakrabarti, S. K., *Phys. Rep.*, **266**, 229, 1996.
Chakrabarti, S. K. and Manickam S. G., *ApJl*, bf 531, L41, 2000.
Chakrabarti, S. K. and Titarchuk, L. G., *ApJ*, **623**, 623, 1995.
Greiner, J., Morgan E. H., & Remillard, *ApJ*, **473**, L107, 1996
Lewin, W. H. G., Jan Van Paradijs, & Taam, R. E., in X-ray Binaries, Eds. Lewin., W. H. G., Jan Van Paradijs, & van den Heuvel, Cambridge: Cambridge University Press, p. 175-232, 1995.
Taam, R. E., Chen, X., & Swank, J. H., *ApJ*, **485**, L83, 1997.
Paul, B., et al., *ApJ*, **492**, L63, 1998.
Yadav, J. S. et al., *ApJ*, **517**, 935, 1999.
Yadav, J. S. and A. R. Rao submitted for publicaiton in *ApJ*, 2000.
Yadav, J. S. Accepted for publication in *ApJ* (2000).

Broadband X-ray Spectroscopy of GRS 1915+105

A. Rau, J. Greiner
Astrophysical Institute Potsdam, 14482 Potsdam, Germany

Abstract. We analyzed RXTE data of GRS 1915+105 of X-ray low states between 1996 and 1998. The X-ray spectrum is dominated by the power law component. We found (i) that the power law is pivoting at 10-30 keV, (ii) that the power law slope correlates with radio flux, (iii) three different groups of 3-10 keV residuals, (iv) that one of these residual groups correlates with the power law slope.

Keywords: X-ray binary, GRS 1915+105, spectroscopy

The prototypical microquasar GRS 1915+105 was discovered by Granat (Castro-Tirado, Brandt & Lund 1992) as a transient X-ray source. Observations with RXTE PCA revealed astonishing X-ray variability (Greiner et al. 1996) which has been classified into a dozen different X-ray states (Belloni et al. 2000).

We analyzed 68 observations from the RXTE public archive of GRS 1915+105 during X-ray low states, so called χ-states (Belloni et al. 2000; no large amplitude variations nor obvious structured variability) from November 1996 to June 1998. For each observation we used PCU 0 data of the PCA and binned HEXTE cluster A data and fitted these with a model consisting of cold absorption (wabs), disk blackbody (diskbb) and reflection (refsch, including a power law) in *XSPEC* with a fixed folding energy of 400 keV and solar abundances. Energies between 4 and 8.5 keV were ignored during the fit.

All reduced X-ray spectra can be divided into three groups depending on the residuals in the energy range 3-10 keV. The first group shows a small hump at 6.4 keV and a dip at 4.5 keV, and the second group has two broad humps at 4.5 and 6 keV. Both groups are mainly seen during the long 1997 low state. The third group has a deep dip at 4.5 keV as the only feature and occurs only at times of radio flares. A deepening of the "dip"-residuals with steeper power law and increasing radio flux is seen, whereas no such trend is visible for the other groups. This correlation between dip depth and radio flares suggests that the depth is connected with the strengths of a possibly nearly-spherical outflow or accretion disk wind (inclination is 70° from radio jet characteristics, e.g. nearly edge-on) where a part may be collimated into a jet.

During χ-states (independent of the three residual groups) an increasing PCA count rate is related to a decreasing HEXTE count rate and an increasing spectral photon index. Interestingly, the power law

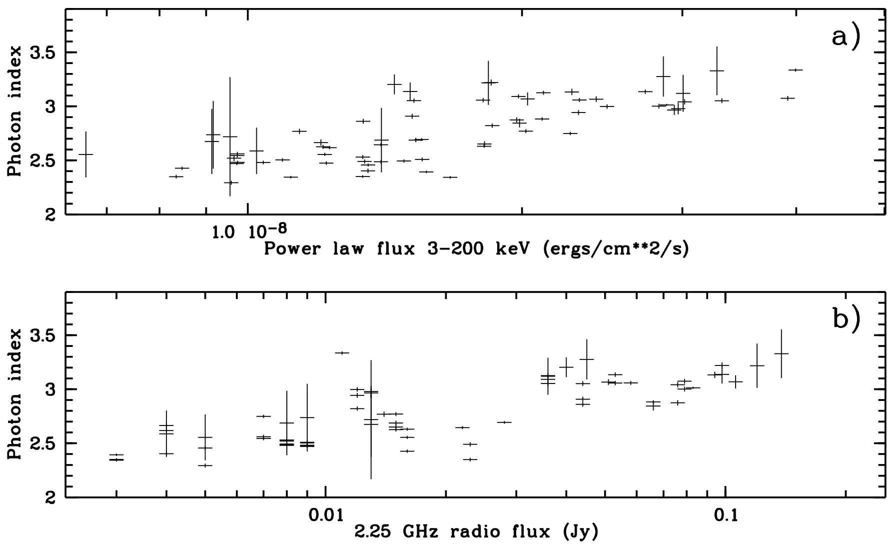

Figure 1. X-ray power law photon index as function of a) the 3-200 keV power law flux and b) the 2.25 GHz Green Bank Interferometer (GBI) radio flux.

pivotes at 10-30 keV, while the disk component is always negligible. Therefore a factor of 3-4 in PCA count rate can be explained by a varying power law flux by the same factor (Fig. 1a). Thus, the power law producing corona of hot electrons can be the origin of the observed count rate variation. An increasing photon index is caused by a decreasing electron temperature in the corona and the observed variation implies a temperature variation between 25 and 50 keV (Sazonov & Sunyaev 2000).

Also correlated with the power law slope is the 2.25 GHz radio flux as measured with the GBI such that a higher photon index (lower electron temperature) is related to higher radio flux (Fig. 1b). This could be due to a shift of the synchrotron radiation to longer wavelengths with decreasing electron temperature. This would be in agreement to a correlation of the K band flux with the X-ray hardness ratio (Greiner et al. 2001).

References

Belloni T., Klein-Wolt M., Mendez M. et al. 2000, *A&A* 355, 271
Castro-Tirado A.J., Brandt S., Lund N., 1992, *IAU Circ.*, 5590
Greiner J., Morgan E., Remillard R.A., 1996, *ApJ*, 473, L107
Greiner J., Vrba F.J., Henden A.A. et al. 2001, these proceedings
Sazonov S.Y., Sunyaev R.A., 2000, *AstL*, 26, 494

Correlations Between the Radio Emission and the X-ray Timing Properties in GRS 1915+105

M. Muno (muno@mit.edu), R. Remillard and E. Morgan
MIT Center for Space Research

E. Waltman
Naval Research Laboratory

R. Hjellming
National Radio Astronomy Observatory

G. Pooley
Mullard Radio Astronomy Laboratory, Cavendish Laboratory

GRS 1915+105 is noted for exhibiting X-ray, radio, and infrared emission which is variable on time scales of seconds to minutes (Mirabel et al., 1998; Eikenberry et al., 1998; Greiner et al., 1996; Belloni et al., 1997). However, the source also exhibits steady emission which is reminiscent of black hole candidates such as Cyg X−1 and GX 339−4. Both the variable and steady X-ray conditions can be seen as transitions between two basic modes of X-ray emission (Muno et al., 1999). The soft state exhibits little X-ray emission above 40 keV and no 0.5–10 Hz quasi-periodic oscillation (QPO) in its power density spectrum (PDS). The hard state exhibits a power law energy spectrum up to at least 100 keV, and a 0.5–10 Hz QPO. Bright (100 mJy at 15 GHz), optically thick radio emission often accompanies the hard state of GRS 1915+105 (Foster et al., 1996), similar to the hard states of Cyg X−1 (Brocksopp et al., 1999) and GX 339−4 (Corbel et al., 2000). This so-called "radio plateau" emission (e.g. MJD 50730-50750 in Figure 1) originates from a compact jet (Dhawan et al., 2000). However, other hard X-ray states are sometimes accompanied by radio emission which is a factor of 10 fainter (see MJD 50440-50560 and MJD 51053-51096 in Figure 1).

During periods of optically thick radio emission, the power contained in the radio-emitting jets may be a significant fraction of the accretion energy which can be inferred from the X-ray emission. This has led Fender et al. (1999) to speculate that the Compton corona responsible for the X-ray power law represents the base of the compact radio jet. This motivates us to examine whether the X-ray spectral and timing properties during the hard state of GRS 1915+105 are related to the intensity of the radio emission.

We have analyzed all 111 *RXTE* PCA and HEXTE observations of GRS 1915+105 during the hard-steady state taken between 1996 April 15 (MJD 50188) and 1999 March 22 (MJD 51259). Radio flux

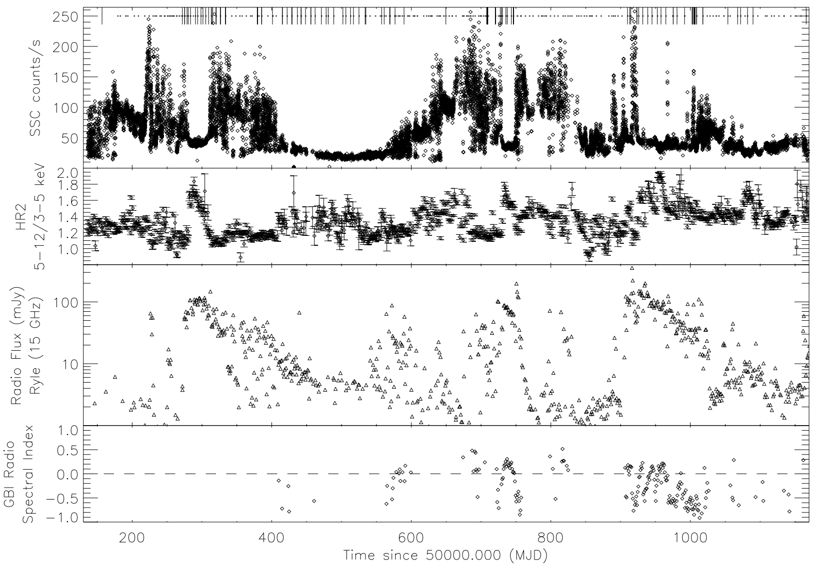

Figure 1. Monitoring data for GRS 1915+105. *Top panel*: 1.5–12 keV light curve from the *RXTE* All-Sky Monitor (ASM). Vertical bars across the top represent hard-steady pointed *RXTE* observations, and dots the remainder of the pointed observations. *Second panel*: *RXTE* ASM hardness ratio HR2 (5-12 keV / 3-5 keV). *Third panel*: Radio flux from the Ryle telescope at 15 GHz. *Bottom panel*: GBI radio spectral index ($\alpha = \Delta \log S_\nu / \Delta \log \nu$) using $\nu = 8$ and 2 GHz; points are plotted only if the flux density at both frequencies was larger than 20 mJy.

densities at 15 GHz from the Ryle telescope occur within a half-day of 98 of these observations, and public measurements of the radio spectral index between 2 and 8 GHz from the NSF-NRAO-NASA Green Bank Interferometer are available for 25 observations. For each *RXTE* observation, we have computed the PDS, Fourier phase lag spectrum, and the coherence function from the PCA data (Nowak et al., 1999). Representative examples of these X-ray timing properties of GRS 1915+105 are displayed in Figure 2.

We find that radio emission always accompanies the hard-steady state of GRS 1915+105, but that the radio flux density at 15 GHz and the X-ray flux between 2–200 keV are not correlated. However, in Figure 3 we demonstrate that as the radio emission becomes brighter and more optically thick, 1) the frequency of a ubiquitous 0.5–10 Hz X-ray quasi-periodic oscillation decreases, 2) Fourier phase lags measured between between hard (11.5–60 keV) and soft (2.5–4 keV) photons in the frequency range of 0.01–10 Hz change sign from negative to positive,

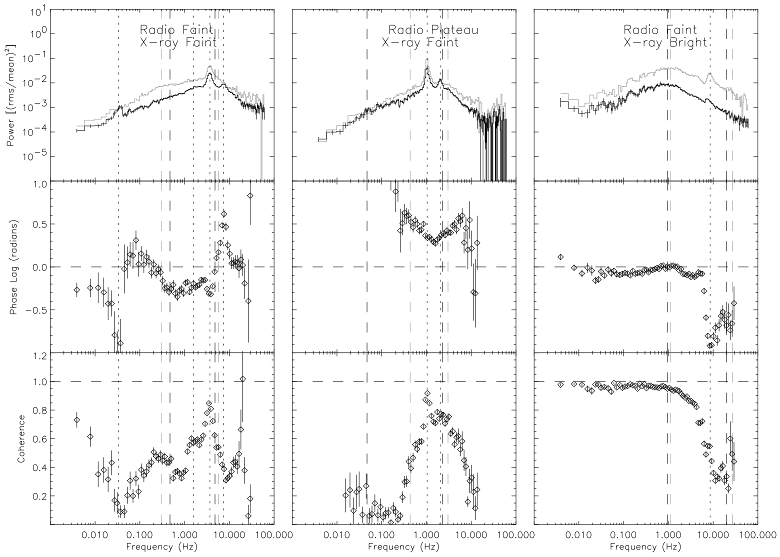

Figure 2. Timing properties of the three variants of the hard X-ray state, from observations on MJD 50488, 50737, and 50708 from left to right. *Top panel*: PDS for the 2–4.3 keV energy band (black lines), and the 11.5-60 keV band (grey lines). *Middle panel*: the phase lags between the 2-4.3 keV and the 11.5–60 keV bands, where positive values indicate hard photons lag soft. *Bottom panel*: the coherence function between the 2-4.3 keV and the 11.5–60 keV bands (a measure of the linearity of the transfer function relating soft and hard signals; see e.g. Nowak et al. 1999) . In all panels, the frequencies of QPOs are shown with black short-dashed lines, and break frequencies with black long-dashed lines. The break frequency in the 11.5-60 keV band is shown with grey long-dashed lines.

3) the coherence between hard and soft photons at low frequencies decreases, and 4) the relative amount of low frequency power in hard photons compared to soft photons decreases.

These correlations provide compelling evidence of a link between the X-ray and radio emitting regions, but it is difficult to interpret the sign shifts in the phase lags and the loss of coherence in the X-ray bands when the radio emission is faint. The radio plateau state of GRS 1915+105 resembles the hard state in Cyg X−1 in that the X-ray phase lags are positive and the radio emission is bright and optically thick, but the low observed coherence in Figure 2 stands in contrast to the high coherence observed in Cyg X−1 (Nowak et al., 1999). Nevertheless, the search for similar trends in other sources may provide insights into the connection between the radio and X-ray emission from binary black hole candidates.

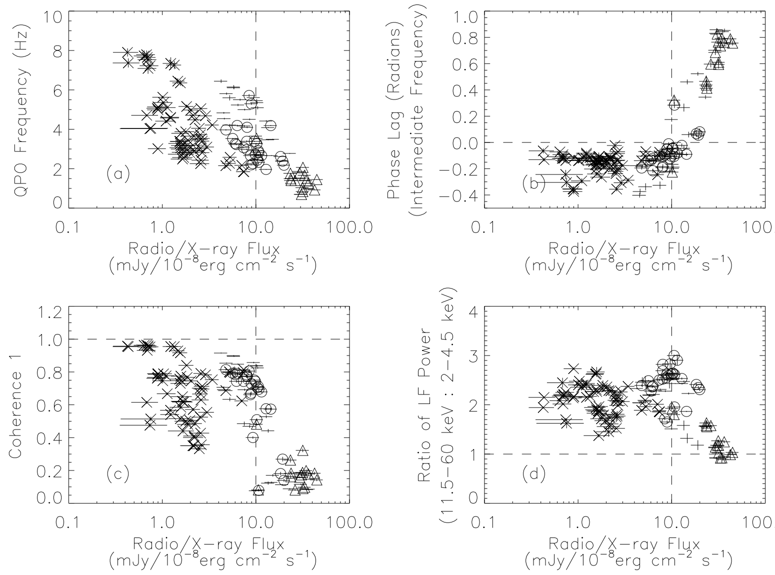

Figure 3. X-ray timing properties as a function of the ratio of radio to X-ray flux. Triangles represent bright ($>$ 15 mJy at 15 GHz) optically thick ($\alpha < -0.2$) conditions, circles bright optically thin conditions, and $\times$'s radio-faint conditions. a) The QPO frequency. b) Phase lags (as in Figure 2) averaged between the low frequency break and the QPO. c) The coherence function (as in Figure 2) averaged over frequencies below the low frequency break. d) The ratio of the integrated broad-band power below the QPO frequency in high (11.5–60 keV) to low (2–4.5 keV) energy bands.

References

Belloni, T., Méndez, M., King, A. R., van der Klis, M., & van Paradijs, J. 1997, ApJ, 479, L145

Brocksopp, C., Fender, R. P., Larionov, V., Lyuty, V. M., Tarasov, A. E., Pooley, G. G., Paciesas, W. S., & Roche, P. 1999, MNRAS, 309, 1063

Corbel, S., Fender, R. P., Tzioumis, A. K., Nowak, M., McIntyre, V., Duroudhoux, P., & Sood, R. 2000, A&A, 359, 251

Dhawan, V, Mirabel, I. F., & Rodríguez, L. F. 2000, ApJ, 543, 373

Eikenberry, S. S., Matthews, K., Morgan, E. H., Remillard, R. A., & Nelson, R. W. 1998, ApJ, 494, L61

Fender, R. P. et al. 1999, ApJ, 519, L165

Foster, R. S., Waltman, E. B., Tavani, M., Harmon, B. A., Zhang, S. N., Paciesas, W. S., & Ghigo, F. D. 1996, ApJ, 467, L81

Greiner, J., Morgan, E. H., & Remillard, R. A. 1996, ApJ, 473, L107

Mirabel, I. F., Dhawan, V., Chaty, S., Rodríguez, L. F., Marti, J., Robinson, C. R., Swank, J., Geballe, T. 1998, A&A, 300, L9

Muno, M. P., Morgan, E. H., & Remillard, R. A. 1999, ApJ, 527, 321

Nowak, M. A., Vaughan, B. A., Wilms, J., Dove, J. B., & Begelman, M. C. 1999, ApJ, 510, 874

Viscous evolution of an accretion disk in a binary system *

Galina V. Lipunova† and Nikolai I. Shakura
Sternberg Astronomical Institute, Moscow State University, Universitetskii pr. 13, Moscow, 119899 Russia (galja@sai.msu.ru)

Abstract. A new analytical solution describing a time-dependent disk in a binary system at outburst, which has a fixed tidally-truncated outer radius, is applied to 1975 X-ray nova burst of A0620-00. The X-ray flux of a multicolor (black-body) α-disk decays quasi-exponentially with time. Modeling the X-ray and the optical light curves of A0620-00, we can estimate α and obtain 'distance–mass of compact object' relation.

Keywords: accretion disk, close binaries, X-ray novae, A0620-00 (=V616 Mon)

We consider the basic viscous diffusion equation (e.g., Lipunova and Shakura, 2000) as applied to accretion disks. This equation shows that the time behaviour of a disk depends on the relation between kinematic coefficient of turbulent viscosity ν, column density of a disk Σ, and radius r.

If ν is a function of radius alone, the basic differential equation of diffusion type is linear. This case was considered by Weizsäcker (1948), Lüst (1952), Lynden-Bell and Pringle (1974).

The general case, when ν is a power–law function of Σ and r, was considered by Filipov (1984; 1988), Lyubarskii and Shakura (1987).

We adopt the $\nu \propto \Sigma^l\, r^m$ relation and pioneer in considering a confined accretion disk. We assume specific outer boundary conditions for a disk in a binary system (Lipunova and Shakura, 2000) and obtain a new solution. The standard α-model of the viscosity is assumed.

The bolometric luminosity is found to vary with time as a power low with an index of $-5/2$, if Thomson scattering dominates the opacity, and $-10/3$, if free-free and free-bound transitions do.

Assuming the spectrum to be a multi-color black body one, the X-ray luminosity is obtained to vary as $\exp\left(-t^{5/6}\right)$. This is quite close to the exponential behaviour.

To illustrate how the parameters of the disk can be obtained, we model the 1975 burst of A0620-00 (Fig. 1). We used the X-ray data in the 3–6 keV band of *Ariel-5* (Kaluzienski et al. 1977) and the data in B and V optical bands (Kuulkers 1998, and references therein).

---

* The work is partially supported by the RFBR grant 00–02–17164, the program 'Universitety Rossii' (grant 5559), and NTP 'Astronomia' grant 1.4.4.1 (Russia)

† GVL is thankful to Instituto de Astrofisica de Andalucia for supporting her visit to Granada. She is also supported by ISSEP.

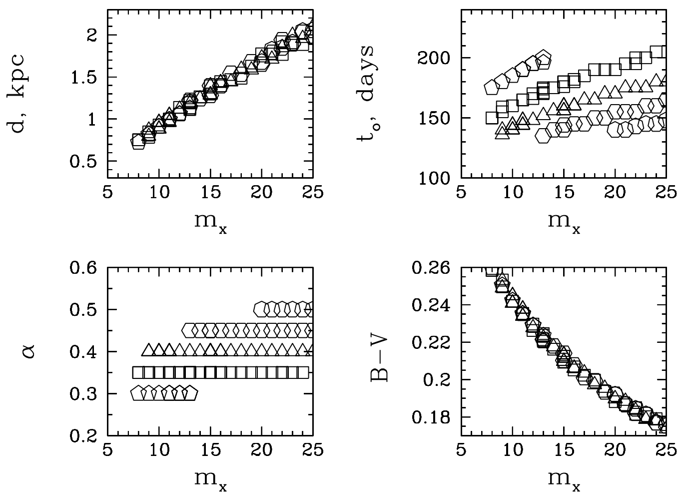

Figure 1. A multitude of models is restricted to the following values of parameters: $m_{\rm x} = M_{\rm BH}/M_\odot = 5 \div 25$, B−V (27th day after peak) $= 0.17 \div 0.26$. We checked the values of α: 0.2, 0.25, 0.3, 0.35, 0.4, 0.45, 0.5, 0.55, 0.6. d is the distance to the source. The right upper panel displays the corresponding values of $t_{\rm o}$ (see Lipunova and Shakura, 2000) if we set t to be the time after the peak of the outburst, MJD 42638.4 = 13/08/1975.

We see that the model is consistent with the idea of a black hole in this binary and with the distance estimates available in literature (Barret et al., 1996; Chen et al., 1997). We choose the models with E(B−V)=0.39 (Wu et al., 1976). From Kuulkers (1998) we have B−V (27 d)= 0.24 (±10%), then BH mass lies in the range 9–14 $M_\odot$.

References

Filipov, L. G. Self-Similar Problems of the Time-Dependent Discs Accretion and the Nature of the Temporary X-Ray Sources. *Adv. Space Res.*, 3:305–313, 1984.

Filipov, L. G. General method describing self-similar regimes of nonstationary disc accretion - A possibility of self-organization. *Adv. Space Res.*, 8:141–150, 1988.

Kaluzienski, L. J., S. S. Holt, E. A. Boldt, and P. J. Serlemitsos. All-Sky Monitor observations of the decay of A0620-00 (Nova Monocerotis 1975). *ApJ*, 212:203–210, 1977.

Kuulkers, E. A0620-00 revisited: a black-hole transient case-study. *New Astronomy Rev.*, 42:1–22, 1998.

Lipunova, G. V. and N. I. Shkura. New solution to viscous evolution of accretion disks in binary systems. *A&A*, 356:363–372, 2000.

Lüst, R. *Naturforschg*, 7(a):87, 1952.

Lynden-Bell, D. and J. E. Pringle. The evolution of viscous discs and the origin of the nebular variables. *MNRAS*, 168:603–637, 1974.

Weizsäcker, C. F. Die Rotation kosmischer Gasmassen. *Naturforschg*, 3(a):524–539, 1948.

The Accretion-Ejection Instability in X-ray Binaries

P. Varnière[†] and M. Tagger
Service d'Astrophysique (CNRS URA 2052) ,CEA/Saclay 91191 Gif sur Yvette

Abstract. The Accretion-Ejection Instability (AEI), which can occur in magnetized disks near equipartition, is a good candidate to explain the low-frequency QPO in black-hole binaries. Here we present analytical work concerning the behavior of QPO frequency and the emission of Alfvén waves from the disk to the corona.

Keywords: accretion, accretion disk, instabilities, MHD waves, galaxies:jets

1. Introduction

The AEI is a spiral instability, similar to galatic spirals but driven by magnetic stress rather than self-gravity. It occurs in the inner region of an accretion disk threaded by a vertical magnetic field of the order of equipartition with the gas pressure. The spiral extracts energy and angular momentum from the disk, causing accretion, and stores them in a Rossby vortex at its corotation radius (see also the contributions of Tagger and Caunt, these proceedings). This vortex then leaks energy and angular momentum as Alfvén waves to the corona, where it can power a wind or a jet. For more details see Tagger,M.& Pellat,R. (1999).

2. QPO Frequency in Pseudo-Newtonian Potential

Relativistic effects change the rotation curve of the disk near the last stable orbit. They allow the existence of an Inner Lindblad Resonance (ILR) for the $m = 1$ mode. This changes the properties of the 1-armed spiral (best candidate to explain the QPO), and therefore its frequency.

We have studied, using a pseudo-newtonian potential, the properties of the instability when the disk inner radius r_{int} approaches the Last Stable Orbit at r_{LSO}. When r_{int} is large the QPO frequency varies as $\omega \propto r^{-3/2}$; but as r_{int} approaches r_{LSO} the correlation changes and becomes *positive* (the QPO frequency decreasing with a decreasing radius) when $r_{int} < 1.4 r_{LSO}$, *i.e.* when the $m = 1$ mode has an Inner Lindblad Resonance in the disk (Varnière,P. , Rodriguez,J. & Tagger,M., 2000). We consider this as a possible explanation for the positive correlation found (contrary to other sources) in GRO J1655 as shown in these proceedings and Rodriguez,J., Varnière,P.& Tagger,M. (2000).

[†] (varniere@cea.fr)

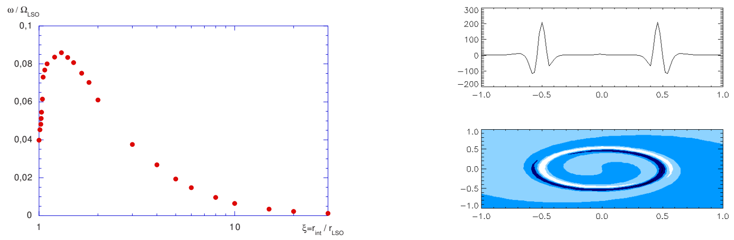

Figure 1. (left) the QPO frequency as a function of the disk inner radius r_{int}. The frequency-radius correlation is reversed when $r_{int} \lesssim 1.4 r_{LSO}$. (right) radial profile and spatial structure of the flux of Alfvén waves emitted to the corona.

3. Emission of Alfvén Waves

The Rossby vortex twists the footpoint of the field lines threading the disk. If the disk has a low density corona this twisting will be propagated upward as Alfvén waves. The energy and angular momentum extracted from the disk will thus be transfered to the corona where they can power a wind or jet. We study this with a variational form

$$F = [\text{energy of the waves}] + i \;\; [\text{outgoing spiral} + \text{ vortex} \\ + k_z \text{ Alfvén Waves}]$$

where imaginary terms correspond to amplification or damping of the instability. From the numerical solution we compute the flux of the emitted Alfvén waves. The result, plotted in Figure 1, shows that it peaks at the corotation radius, where the Rossby vortex is localized.

4. Conclusions

The frequency of the AEI, and its variations with the disk inner radius, make it a very good candidate to explain the “ubiquitous” QPO. The accretion energy and momentum extracted from the disk are propagated to the corona as Alfvén waves.

References

Rodriguez,J. , Varnière,P. & Tagger,M. Accretion-Ejection Instability and QPO: II. Observations. submitted to A&A

Tagger,M. & Pellat,R. Accretion-Ejection Instability in Magnetized Disks. *AA*, 2:155–192, 1999.

Varnière,P. , Rodriguez,J. & Tagger,M. Accretion-Ejection Instability and QPO: I. Theory. submitted to A&A

The Accretion Ejection Instability : Observational Tests

J. Rodriguez (jrodriguez@cea.fr), P. Varnière, M. Tagger and Ph. Durouchoux
Service d'Astrophysique (CNRS URA 2052) ,CEA/Saclay 91191 Gif sur Yvette

1. First Steps : GRO J1655-40

QPOs are commonly considered to originate in the disks of X-ray binaries. One thus expects, and most often observes, that the QPO frequency decreases as the disk inner radius increases. However Sobczak *et al.* (1999) pointed out an opposite behavior in the case of GRO J1655-40. This might prove usefull in testing the theory of the Accretion-Ejection Instability (see contributions by Caunt, Tagger and Varnière, these proceedings). At the same time, Merloni, Fabian, and Ross (1999) showed that, when fitting the sources spectra with the standard model (multicolor blackbody+ power law), severe distorsions could be due to the vertical structure of the disk. In that view we re-did the spectral analysis of the observations in which Sobczak *et al.* found QPO's.
Using the criterion of Merloni *et al.* , we find that all the data points from GRO J1655-40 where the fits give an anomalously low inner radius must be excluded. The remaining points confirm the inverse correlation.

2. Another Good Candidate : GRS 1915+105

Because of its high and rapid variability, and following the results found by Markwardt et al., 1999, and Muno et al., 1999, we then focussed on GRS 1915+105. In particular we studied very precisely two 30 min cycles present in the observation of September 9^{th} 1997, in which the QPO frequency had been seen to vary (Markwardt *et al.* , 1999, Swank *et al.* , 1997), correlated to the flux, the color temperature and the color radius itself.

We extracted, during two $\sim 30min$ dips, every 20s a 16s spectrum and a lightcurve, extracting both the QPO frequency and the spectral parameters (Rodriguez *et al.* , 2000).

We have also analyzed recent observations of GRS 1915+105, pointed as a target of opportunity, on April $17^{th}, 22^{th}, 23^{th}$ by RXTE. Although only the first date showed high variability, in the three observations a strong QPO, together with its first harmonic are highly correlated to the flux (work in progress).

3. Results and Interpretation

- Applying more stringent criteria leads us to exclude some of the data points observed by Sobczak *et al.* in GRO J1655-40, but the points we retain do show the inverse correlation between the QPO frequency and the disk inner radius.
- Though highly variable GRS 1915+105 does not present this inverse correlation, during the 30 mn cycles.
- These observations are compatible with the theory of the Accretion-Ejection Instability (see Varnière., these proceedings), if the disk of GRO J1655-40 is always near the Last Stable Orbit when QPO are observed, and the disk of GRS 1915+105 never approaches it during its 30 mn cycles.
- The criterion of Merloni et al. leads us to exclude the data points of GRO J1655-40 where the spectral fits return a very low color radius($\sim$ very few kms). But we find that these points are not compatible with the predictions of Merloni, as they systematically show a higher temperature when the color radius decreases. On the other hand, data points at the onset of the low state, in GRS 1915+105, are compatible with the predictions of Merloni *et al.* .
- We note that in GRO J1655-40, as well as during the hard-steady state of GRS 1915+105, the very low color radius actually means a small size of the emitting region. This and the higher temperature would be compatible with the presence in the disk of a spiral shock or hot point, where accretion energy would be dissipated.

References

Markwardt, C.B., Swank, J. H. & Taam R. E. *ApJ*, **513**, L37, 1999
Merloni, A., Fabian, A. C. & Ross, R. R. *MNRAS*, **313**, 193M, 2000
Rodriguez, J., Varnière, P., Tagger, M., & Durouchoux, Ph. submitted to *A&A*
Sobczak, G. J., McClintock, J. E., Remillard, R. A., Cui, W., Levine, A. M., Morgan,E. H., Orosz, J. A. & Bailyn, C. D. *ApJ*, **531**, 537S, 2000
Tagger, M. & Pellat, R. *A&A*, **349**, 1003, 1999
Varnière, P., Rodriguez, J. & Tagger, M. submitted to *A&A*

Analytical solutions of accretion disks with outflows

W. Kluźniak
Copernicus Astronomical Center, ul. Bartycka 18, 00-716 Warszawa, Poland

Abstract. Analytical solutions of accretion flow in three dimensions are discussed, with the flow restricted to be axisymmetric. Steady outflows are a generic feature for many classes of solutions. Many two-dimensional numerical solutions of accretion exhibit non-trivial flow structure in agreement with our results. Another mechanism of driving outflow is the well-known propeller mechanism, could it be responsible for the behaviour of GRS 1915+105?

Keywords: accretion, outflow

1. On accretion disk solutions

Analytical considerations in the literature are usually essentially one-dimensional (e.g. the radial structure of accretion disks is determined by solving a set of height-averaged equations, while the vertical structure is found at a fixed radius).

Hydrodynamic flow in accretion disks is intrinsically two-dimensional or even three-dimensional. Perhaps for this reason, it is fashionable and useful to model accretion flows and jet outflows numerically. Most of these simulations are two-dimensional, they are carried out in a limited domain (i.e., the results may depend on the boundary conditions adopted), and frequently it is not clear whether a steady state has been reached, or whether the solution is transient.

It would, then, be worthwile to expend more effort on obtaining analytical results in two or three dimensions. In fact, nearly exact analytical results can be obtained, and the effort expended is immediately rewarded with novel results which only subsequently are also uncovered numerically. For lack of space, I will give but one example: analytical work has clearly shown outflow in the plane of the disk (Urpin 1985, Kluźniak and Kita 2000), such outflow is discerned also in many numerical simulations (e.g., Igumenshchev and Abramowicz 1999, Lee 2000).

2. GRS 1915+105, an accreting pulsar?

It is almost universally assumed that GRS 1915+105, the micro-quasar with bizarre light-curves, is a black hole. Thus, work on understanding the outflows associated with radio emission, usually focuses on possible ejection of material from the inner parts of a black-hole accretion disk. But the mass of the source is not known, and it is quite possible that the powerhouse is a rotating magnetized neutron star in a state of intermittent accretion.

The unusually steady (in frequency) quasi-periodic oscillation is strongly suggestive of a pulsar. Several contributions to this volume discuss the characteristic transitions between two or three accretion states of GRS 1915+105. It seems to me, that these are about what would be expected of an accreting pulsar at a period which is the inverse of the QPO frequency. It is accepted in neutron star theory, that a rotating magnetized neutron star can accrete matter only if the mass penetrates the corotation radius (where, by definition, the keplerian period is equal to the stellar period), this is possible only above a certain mass accretion rate. Otherwise matter is expelled.

The corotation radius for such a pulsar, as well as the radius of the light cylinder, comes out to be very close to the inner radius of the disk (inferred from observations and reported in several contributions in this volume, e.g., Belloni 2000) of GRS 1915, in that state which is accompanied by strong radio emission, while the disk radius in the radio-quiet state is much smaller [although other spectral models do not support this interpretation, Vilhu 2000].

Obviously, this model has the great advantage that it connects one observed number (the QPO frequency) with another (inner disk radius), and correlates in a natural way one state of the system with expulsion of matter and radio activity (which is quenched in the other state by accretion onto the neutron star). Were the black hole models equally successful! The QPO frequency should be monitored over the years—it is likely to decrease on the pulsar model, as much of the source luminosity is powered by the kinetic energy of the rotating star.

Acknowledgements

This work was supported in part by KBN grant 2P03D 004 18.

References

Belloni, T., 2000, this volume
Igumenshchev, I. V.; Abramowicz, M. A, 1999, MNRAS, 303, 30
Kluźniak, W., Kita, D. 2000, astro-ph/0006266
Lee, W. 2000, this volume
Urpin, V. A., 1984, AZh, 61, 84 [SvA, 28, 50]
Vilhu, O. 2000, this volume

Advection dominated flows around black holes in two dimensions.

William H. Lee
Instituto de Astronomía, UNAM
Apdo. Postal 70–264, Cd. Universitaria, México D.F. 04510, México

Abstract. We show the results of two–dimensional, azimuthally symmetric simulations of advection dominated fluid flows around black holes. We use the SPH method, and the α–prescription for the viscosity, including all terms in the stress tensor. We have performed calculations with $0.001 < \alpha < 0.2$ and find strong circulation patterns in the flow, on spatial scales that depend on the magnitude of the viscosity.

Keywords: accretion disk, hydrodynamics

1. Introduction, method and initial conditions

The astrophysical relevance of accretion flows in which radiative cooling is inefficient has been recently emphasized (Narayan and Yi, 1994). These flows show complicated hydrodynamical behavior that is very different from that obtained with the thin disk approach (Shakura and Sunyaev, 1973) for efficient cooling.

We use the Smooth Particle Hydrodynamics (SPH) method (Monaghan, 1992), in azimuthal symmetry. The equation of state is $P = \rho u(\gamma - 1)$ with $\gamma = 4/3$. Viscosity is computed using an α prescription ($\mu = \alpha\rho c_s^2/\Omega_k$), including all the terms from the viscous stress tensor. The black hole is modeled as a Newtonian point mass with an absorbing boundary at $r_{in} = 1.3 r_G = 1.3(2GM_{BH}/c^2)$. We use two kinds of initial conditions: 1) equilibrium hydrostatic tori with constant specific angular momentum; 2) matter injection at a steady rate at a radius $r = 300 r_G$. We assume no radiative energy losses.

2. Results

For initially hydrostatic tori, the presence of a hot, high–entropy bubble near the equatorial plane is easily seen (Figure 1). This moves outward in the disk, on top of a background accretion flow. There is a large–scale circulation pattern, on a scale $z \simeq r$. For a lower viscosity $\alpha = 0.001$ there are small–scale vortices in the disk, and the overall behavior is more turbulent. A background accretion flow is also present.

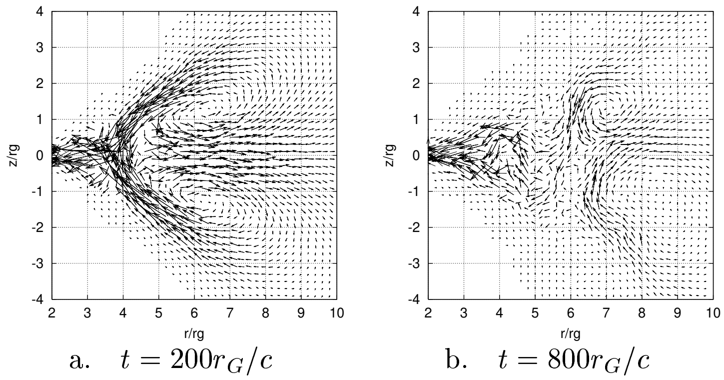

Figure 1. Momentum vector field $\rho\vec{v}$ for $\alpha = 0.01$.

For the case of matter injection, the flow structure is governed by the magnitude of the viscosity, with small–scale eddies at low values of α and large–scale circulations when the viscosity is high. The fluid shows significant oscillations in the vertical direction as it moves radially inward.

With these simulations we have tested our code with previously published results obtained with a different numerical scheme (Igumenshchev et al., 1996; Igumenshchev and Abramowicz, 1999), and we have found excellent agreement both in a qualitative and quantitative manner. In future work we will extend our results to study the parameter space (α, γ) and increase the resolution.

Acknowledgements

I acknowledge support from CONACyT (27987E), DGAPA (IN-119998) and helpful conversations with M. Abramowicz and W. Kluźniak.

References

Igumenshchev I. V. Chen X. and M. A. Abramowicz. Accretion disks around black holes: two–dimensional, advection cooled flows. *MNRAS*, 278:236–250, 1996.

Igumenshchev I. V. and M. A. Abramowicz. Rotating accretion flows around black holes: convection and variability. *MNRAS*, 303:309–320, 1999.

Monaghan, J. J. Smoothed Particle Hydrodynamics. *Ann. Rev. Astron. Astrophys.*, 30:543–574, 1992.

Narayan R. and I. Yi. Advection–dominated accretion: a self–similar solution. *ApJ*, 428:L13–L16, 1994

Shakura I. N. and R. A. Sunyaev. Black holes in binary systems. Observational appearance.. *A&A*, 24:337–355, 1973.

Formation and dynamics of neutron haloes in disk accreting black holes

E.V. Belyanin, A.A. Derishev
Institute of Applied Physics, 46 Ulyanov St., 603600 Nizhny Novgorod, Russia

Keywords: accretion disk, black hole, gamma-ray

There are many theoretical and observational indications that the hot plasma of ion temperature T_i exceeding several MeV can exist in the inner accretion disks around black holes. Formation of two-temperature region with $T_i > T_e$ in accretion disks has been predicted as long ago as in 1976 (Shapiro et al., 1976). When the energy transfer from ions to electrons is slow as compared with accretion timescale, the accretion flow becomes nearly adiabatic, and the ion temperature can reach virial values. This idea has led to the prediction of advection-dominated accretion flows which seems to find support in observations of several X-ray transients (Narayan and Yi, 1996).

The presence of hot ions in accretion disks leads to the rich variety of inelastic nuclear interactions. The most prominent of them is neutron production which primarily occurs through dissociation of helium nuclei. This process has potentially important observational implications arising e.g. from possibility of radiative neutron capture with subsequent formation of gamma-ray lines (Aharonian and Sunyaev, 1984).

Neutron production in accretion disks was considered several times (Aharonian and Sunyaev, 1984; Guessoum and Kazanas, 1989) under the assumption that neutrons are quickly thermalized in the disk and are advected to the black hole with the same rate as protons. In this case the neutron fraction in the accretion flow is inevitably small and the radiative-capture gamma-ray lines are weak and smeared out by hot rapidly rotating disk. However, the above assumption is not true if the proton density in the disk is sufficiently low. In this case, as shown in Derishev and Belyanin (2000), the neutron and ion components in the disk effectively decouple, allowing for the accumulation of neutrons. Such a pile-up can lead to much larger neutron number than in previously considered cases.

It is important that, once formed, such a halo becomes self-sustained. This means that, even if the ion temperature in the disk falls below the threshold for He dissociation by protons, the neutron production is supported by collisions of energetic neutrons from the halo with helium nuclei. The self-sustained mode implies that at least one of three neutrons resulting from helium dissociation breaks another helium nucleus before decaying or being advected into the black hole. These two possibilities provide, respectively, lower and upper bounds on the range of accretion rates in which the self-sustained neutron halo may exist.

Our analysis shows (Derishev and Belyanin, 2000) that neutron halo exists in a broad range of disk parameters and can lead to a number of important observational and dynamical effects. In particular, neutron haloes can be the natural source of relativistic electrons and positrons produced in proton-neutron and neutron-neutron collisions. In the presence of abundant soft X-rays from disk, relativistic electron-positron pairs are quickly cooled, and the snapshot of electron distribution would demonstrate that the majority of them has energies between 50-500 keV. The resulting spectrum above 100 keV has a typical comptonization pattern. Pair cascade, if developed, leads to a hard power-law tail with index around 2. Both features are frequently observed in the hard state of accreting black-hole candidates. In addition, very hard radiation should be present with photon energies up to 70 MeV. However, it is expected to contain much less energy than hard X-rays and is difficult to observe. Deuterium gamma-ray line at 2.2 MeV resulting from neutron capture is also expected at a level detectable by future INTEGRAL mission.

Furthermore, the presence of neutron halo strongly affects the dynamics of accretion and leads to the rich variety of transient dynamical regimes.

Acknowledgements

This work has been supported by Russian Foundation for Basic Research (the project 99-02-18244) and by the Russian Academy of Science through a grant for young scientists.

References

Aharonyan, F. A. and R. A. Sunyaev. *Monthly Notices RAS*, 210:257, 1984.
Derishev, E. V. and A. A. Belyanin. *Astron. & Astrophys.*, submitted.
Guessoum, N. and D. Kazanas. *Astrophys. J.*, 345:356, 1989.
Narayan, R., J. McClintock, and I. Yi. *Astrophys. J.*, 457:821, 1996.
Shapiro, S. L., A. P. Lightman, and D. M. Eardley. *Astrophys. J.*, 204:187, 1976.